Satellite-Based Economic Development Mapping with DeepLabV3+: A Case Study of Cairo

Salma Al Emrany Omar Fouad Youssef Aboukhatwa

A report submitted as part of the requirements for the degree
of Data Science
at the School of Sciences
The American University in Cairo
Cairo, Egypt

June 2025

Supervised By Dr. Noha Youssef

Abstract

Understanding and forecasting economic development at fine spatial resolutions is vital for informed policy-making, equitable resource allocation, and sustainable urban planning. In this study, we present a data-driven, satellite-based framework for mapping and predicting regional economic activity using multispectral Landsat imagery and nighttime lights data from the VIIRS sensor. The research focuses on the Cairo metropolitan region and evaluates temporal trends from 2015 to 2025. A composite dataset was developed by integrating surface reflectance bands, vegetation and water indices (NDVI, NDWI, NDBI), and spatial infrastructure densities derived from OpenStreetMap layers. These inputs were meticulously preprocessed in ArcGIS Pro and standardized with robust NoData handling and UTM projection alignment.

To model the spatial-economic relationships, we designed and trained a DeepLabV3+ regression model with a ResNet-34 backbone, fine-tuned on 2021 Cairo data. The model was tasked with pixel-wise prediction of VIIRS radiance intensity, a widely accepted proxy for local economic activity. The training pipeline was built and executed in Google Colab using PyTorch, with rigorous data tiling, normalization, and augmentation to mitigate overfitting. Model training employed Mean Squared Error (MSE) loss and spanned 30 epochs, achieving convergence with a final validation loss of 40.13.

Predictions were generated for 2023 (test), 2025 (future forecast), and retrospective years including 2019, 2020, 2022, and 2024. Evaluation against true VIIRS imagery revealed strong predictive performance in most years, particularly for 2023 and 2024, where the model achieved R^2 scores of 0.8207 and 0.7742, respectively. However, earlier years such as 2019 exhibited lower R^2 values due to increased noise, changing land use dynamics, and weaker feature generalization.

Throughout the project, extensive preprocessing challenges were encountered and resolved, especially regarding missing values, corrupted raster bands, and composite misalignment. Several iterations were required to re-engineer the ArcGIS Pro pipeline for correct raster mosaicking, index calculations, and density raster generation. Custom

automation scripts were developed to apply consistent NoData values (-9999), project all layers to WGS 84 / UTM Zone 36N, and generate final multi-band composites compatible with deep learning workflows.

This work demonstrates the feasibility and scalability of using a deep learning-based regression model to predict economic development from satellite imagery, even in the absence of ground survey data. The trained DeepLabV3+ model offers interpretable, continuous predictions of urban brightness patterns, potentially enabling policymakers and researchers to monitor growth, detect disparities, and assess development efforts in near-real time. Future extensions may include temporal modeling, multi-region generalization, or multi-task learning setups to improve robustness across diverse geographies and socioeconomic contexts.

Acknowledgements

First and foremost, we are profoundly grateful to Dr. Noha Youssef, whose unwavering support, insightful feedback, and consistent encouragement made this thesis possible. Dr. Noha not only guided us academically, but also believed in the potential of this research when it was merely an ambitious idea. Her patience, understanding, and mentorship throughout the year have been invaluable, and we could not have asked for a more inspiring advisor.

To the Data Science faculty at the American University in Cairo, we extend our sincere thanks for fostering an environment that challenged us, inspired us, and gave us the tools to bring this research to life. Every course, conversation, and consultation contributed meaningfully to the skills we applied throughout this work.

We are deeply thankful to our families for their unconditional love, patience, and belief in us. Thank you for understanding the long hours, the stress, the silence, and the obsession over maps and model metrics. Your support formed the foundation of everything we accomplished.

We would also like to acknowledge the developers and maintainers of the open-source tools and platforms that powered this thesis. In particular, we are indebted to the creators of Google Colab, PyTorch, segmentationmodelspytorch, Rasterio, and ArcGIS Pro. This research could not have been realized without the accessibility, flexibility, and power of these technologies.

Lastly, we want to recognize our past selves, who, even when overwhelmed with uncertainty, never stopped pushing forward. From broken model architectures and GPU crashes to geospatial mismatches and evaluation pitfalls, every challenge shaped us into more capable and determined researchers.

This thesis was not just a research project. It was a shared journey of learning, resilience, and growth, and we are truly grateful for every moment of it.

Contents

List of Tables

List of Figures

Chapter 1

Introduction

In a world increasingly driven by data, the need to understand how cities and regions are growing, economically, socially, and physically, is more important than ever. Traditionally, we rely on sources like national censuses, household surveys, or GDP statistics to measure development. However, these tools are often slow, outdated by the time they are published, and lack the detail needed to understand what's happening in specific neighborhoods or districts. This is especially challenging in fast-growing urban areas where conditions change rapidly. To address this gap, this thesis explores a modern alternative: using satellite images and machine learning to visualize and even predict patterns of economic development across space and time.

Our research focuses on Cairo, Egypt, a megacity that has witnessed enormous growth, stark contrasts in development, and major urban transformations in recent years. We propose a system that can analyze Cairo's changing landscape using publicly available satellite data and turn it into detailed maps that reflect local levels of economic activity. Unlike traditional statistics that tell us what has already happened, our system is designed to not only analyze the present but also map what future development might look like.

This is made possible by combining two types of data captured from space:

- The first is called VIIRS nighttime lights, which measures how brightly different parts of the Earth shine at night. Areas with more light usually indicate more human activity, such as homes, businesses, and infrastructure. This is widely accepted as a good proxy for economic development.
- The second is Landsat imagery, which captures what the Earth looks like during the day across different light wavelengths. Each "band" in this imagery captures

a specific type of light, some visible to the human eye, some not. For example, some bands help us see vegetation health, urban materials, or water bodies. These bands are like layers of information, and by combining them, we can understand land usage patterns and detect early signs of development.

To make this data more meaningful, we also calculated specific indicators from the Landsat imagery:

- NDVI shows the amount of green vegetation.
- NDWI detects water presence.
- NDBI highlights built-up, urbanized areas.

We also included maps of road networks and point-of-interest (POI) densities, such as schools, shops, or hospitals, using open-source mapping data. All of this information was brought together into a final, rich dataset that reflects both the natural and built environment in each area.

The core of our solution is a machine learning model, specifically a DeepLabV3+ deep learning model, a type of artificial intelligence that learns patterns from data. We trained the model to look at these satellite inputs and learn how they relate to actual brightness levels at night, based on past data. Once trained, the model was able to generate new maps showing where development is likely to grow. We tested it on real-world data from multiple years, 2019, 2020, 2022, 2023, and 2024, to ensure accuracy. Then, we used it to map economic activity in 2025, even though that year's nighttime light data doesn't exist yet.

This project makes three major contributions:

1. It provides a tool that can generate high-resolution, city-level development maps in places where reliable economic data is limited or outdated.
2. It demonstrates how artificial intelligence can be used to learn from satellite images and generate continuous predictions, not just categories.
3. It offers a fully reusable and adaptable system that can be applied to other cities or regions, making it useful for governments, urban planners, and researchers alike.

Our journey wasn't smooth. We encountered many technical challenges, such as incomplete satellite data, corrupted files, misaligned maps, and inconsistent values. But each problem led to a better system. We developed a detailed data processing pipeline in ArcGIS Pro (a geographic analysis software) to clean, align, and prepare our data

consistently. We also improved our model's accuracy by adjusting how we handled missing values and selecting the right evaluation techniques.

Ultimately, this thesis responds to a timely question: How can we use technology to understand where our cities are heading, even before the data is officially available? Our answer is a robust, scalable, and transparent system that combines satellite data with machine learning to visualize and anticipate patterns of economic development. We hope that our work can support smarter urban planning, better resource allocation, and more inclusive growth, both in Cairo and beyond.

Chapter 2

Literature Review

Understanding the spatial dynamics of economic development has long been a central concern in urban planning, economics, and policy-making. Traditional approaches, although foundational, often fall short of capturing the fine-grained, rapidly evolving nature of modern urban landscapes. Recent advances in remote sensing and deep learning offer promising alternatives. This chapter reviews the relevant literature on economic measurement techniques, the use of satellite imagery in development studies, and the application of machine learning in spatial prediction.

2.1 Traditional Methods of Measuring Economic Development

Conventional methods of assessing economic activity include the use of national accounts, population censuses, household surveys, and statistical indicators such as Gross Domestic Product (GDP) or income per capita. While these approaches provide vital macroeconomic insights, they suffer from key limitations: they are infrequent, expensive to conduct, often outdated by the time of publication, and spatially coarse, typically limited to the national or governorate level.

As cities grow more complex and heterogeneous, policy decisions require more localized, up-to-date data. In particular, urban development in the Global South often proceeds at a pace that outstrips the frequency and resolution of official statistics. These challenges have driven interest in alternative data sources that can capture economic dynamics with greater spatial and temporal granularity.

2.2 Nighttime Lights as a Proxy for Economic Activity

A significant body of literature has established the use of satellite-derived nighttime light (NTL) data, particularly from the Defense Meteorological Satellite Program (DMSP-OLS) and the Visible Infrared Imaging Radiometer Suite (VIIRS), as a reliable proxy for economic activity. Henderson et al. (2012) were among the first to demonstrate a robust correlation between NTL intensity and GDP, laying the groundwork for its widespread use in economic and development research.

NTL data is especially valuable in contexts with weak or unreliable economic statistics. Because it captures electricity usage, infrastructure density, and human activity, it has proven effective in estimating informal economic growth, urban expansion, and disaster recovery. However, NTL data is not without challenges. Issues such as light saturation in dense urban cores, contamination from fires or moonlight, and the difficulty of distinguishing between different sources of illumination limit its interpretability. Despite these limitations, it remains a central tool in spatial economic analysis.

2.3 Daytime Imagery and Spectral Indices for Urban Analysis

Daytime satellite imagery, particularly from the Landsat program, offers complementary insights into land use, vegetation cover, and built-up area detection. The ability to compute spectral indices such as the Normalized Difference Vegetation Index (NDVI), Normalized Difference Built-up Index (NDBI), and Normalized Difference Water Index (NDWI) enables researchers to characterize the physical environment in ways that relate indirectly to economic activity.

Several studies have used these indices to track urban sprawl, assess agricultural health, and monitor environmental change. For example, Singh et al. (2015) used Landsat and NDVI to quantify urban growth in Indian megacities, while Yao et al. (2020) combined NDVI and NDBI to model poverty across different land-use zones. These indices help capture heterogeneity in urban morphology that may correlate with socioeconomic outcomes, although they do not directly measure economic variables.

2.4 Deep Learning in Remote Sensing

With the rise of deep learning, particularly convolutional neural networks (CNNs), remote sensing has undergone a methodological transformation. CNNs are now widely used for classification tasks in geospatial analysis, including land cover segmentation,

disaster detection, and agricultural monitoring. Architectures such as U-Net and DeepLabV3+ have shown exceptional performance in pixel-level tasks.

In most applications, however, these models are used for classification (e.g., identifying water bodies, buildings, or roads) rather than regression. Using deep learning for predicting continuous variables, such as economic brightness from multispectral inputs, remains less explored, particularly in urban economic contexts. The adaptation of segmentation models like DeepLabV3+ for regression tasks offers a novel direction that combines spatial structure learning with the ability to make continuous, fine-grained predictions.

2.5 Satellite + Machine Learning for Economic Prediction

Several recent studies have begun to bridge the gap between remote sensing and economic modeling through machine learning. Jean et al. (2016) pioneered the use of CNNs trained on daytime satellite imagery to predict poverty in sub-Saharan Africa, achieving high accuracy by learning from both spatial and visual features. Tingzon et al. (2021) extended this approach by integrating VIIRS brightness, Landsat features, and mobile phone data to infer economic well-being in data-scarce regions.

These studies demonstrated that it is possible to infer socioeconomic indicators from imagery, even in the absence of survey data. However, they generally focus on national or regional scales and often require ancillary data that may not be available in all settings. Moreover, they typically aim to predict categorical or aggregated variables, such as poverty deciles or asset ownership, rather than high-resolution continuous outputs like pixel-level nightlight intensity.

2.6 Identified Gaps in the Literature

Despite the growing body of research at the intersection of remote sensing and economic geography, several gaps remain:

* Most existing models are trained for classification rather than continuous regression. * Temporal generalization across years is rarely tested in urban economic forecasting. * Few studies combine multispectral imagery, infrastructure data, and NTL into a unified deep learning model. * Pixel-level predictions at city-scale, especially in the Middle East and North Africa (MENA), are underrepresented. * Very few works utilize the DeepLabV3+ architecture for regression applications in an urban development context.

This thesis addresses these gaps by proposing a deep learning-based regression framework that fuses Landsat imagery, spectral indices, and OSM-derived urban infrastructure layers to predict VIIRS radiance at the pixel level across time. It contributes a novel application of semantic segmentation models to spatial economic prediction, with a focus on temporal generalization and policy relevance in Cairo, Egypt.

Chapter 3

Data Description

This study relied on two main types of satellite data, daytime images that show the land surface and nighttime images that show how brightly different areas are lit after dark, along with map-based information from OpenStreetMap (OSM). Together, these layers were combined to form a comprehensive, year-by-year picture of Cairo's physical and economic environment. Each dataset played a key role in helping us analyze and predict patterns of development.

3.0.1 Landsat Satellite Imagery (Daytime Observations)

The first major data source was Landsat imagery, which captures how the Earth's surface looks from space during the day. These images are collected by the Landsat 8 and Landsat 9 satellites, operated by NASA and the U.S. Geological Survey (USGS). Landsat satellites take pictures of the Earth in multiple "bands," each of which captures a different type of light, some we can see with our eyes (like red or green) and others we cannot (like infrared).

We used seven bands (B1 to B7) in total:

- **B1 (Coastal):** Helps with haze removal and atmosphere corrections.
- **B2–B4 (Blue, Green, Red):** These represent natural colors, useful for viewing landscapes.
- **B5 (Near-Infrared):** Sensitive to healthy vegetation.
- **B6 & B7 (Shortwave Infrared):** Reveal urban materials, soil moisture, and heat patterns.

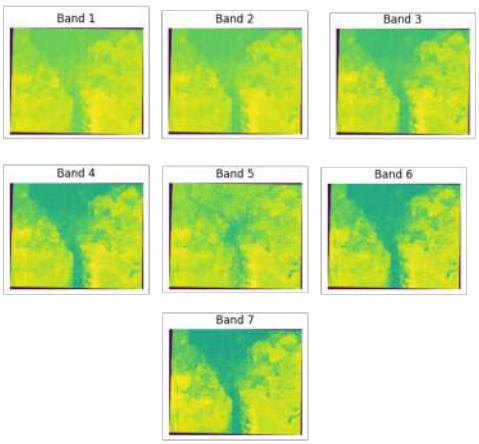

Figure 3.1: 7 Landsat Bands Sample

How the Landsat Data Was Collected

To download this imagery, we used the USGS EarthExplorer platform. Since satellites don't take a picture of the entire city in one go, Cairo is usually covered by two different image tiles, each representing a part of the city. These tiles must be carefully selected based on:

- **Date:** We chose scenes from the same time of year to avoid seasonal differences.
- **Cloud coverage:** We filtered for scenes with less than 5% cloud to make sure the land was clearly visible.
- **Spatial extent:** Only tiles that covered the full Cairo region were selected.

We downloaded images for each year between 2018 and 2025, one pair of tiles per year, each containing all seven bands. Each file was in raster format, essentially a pixel-based image where each pixel contains a numeric value representing the intensity of light for that band.

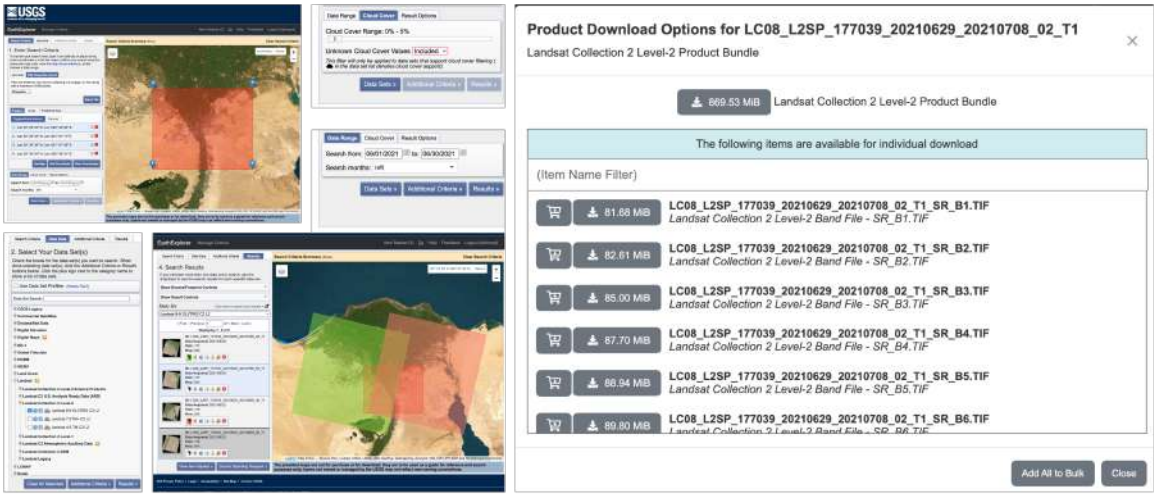

Figure 3.2: Landsat Data Collection Steps

What We Did After Downloading

Once the Landsat images were downloaded:

1. **Mosaicking:** We combined the two tiles (North Cairo + South Cairo) into one image to create full coverage of the city.

2. **Clipping:** We trimmed the images to include only the area inside Cairo's boundaries using a digital map (called a shapefile) of the city.

3. **Fixing NoData Values:** Satellite images often contain missing or invalid pixels. We replaced all of them with the special value -9999, which tells our model to ignore those areas.

4. **Standardizing Projection:** All images were reprojected to a map coordinate system called UTM Zone 36N, which allows for precise distance and area calculations.

3.0.2 Spectral Indices (Derived Layers)

From the cleaned Landsat bands, we generated three special indicators, called spectral indices, that help describe what kind of land is present in each pixel:

- NDVI (Normalized Difference Vegetation Index): Measures how "green" an area is. Higher values mean more healthy vegetation.
- NDWI (Normalized Difference Water Index): Highlights water bodies like rivers or lakes.
- NDBI (Normalized Difference Built-up Index): Detects man-made surfaces like concrete, rooftops, and roads.

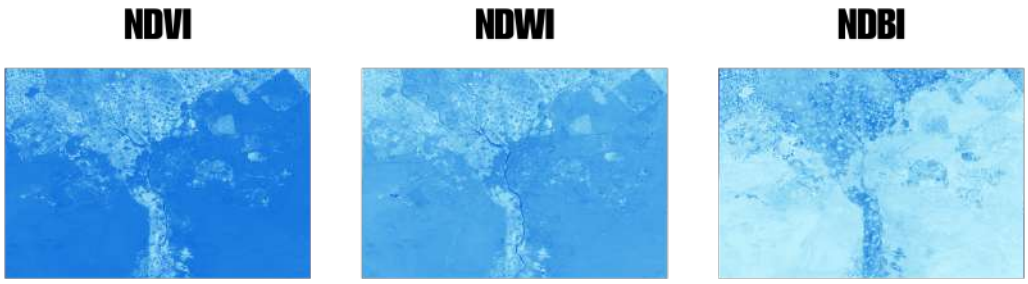

Figure 3.3: Indices Sample

These indices were calculated using formulas that compare the brightness of different bands. For example, NDVI uses the red and near-infrared bands to determine plant health. These layers helped the model recognize different environments, such as farmlands versus dense urban centers.

3.0.3 OpenStreetMap Infrastructure Data (Urban Density Maps)

To measure infrastructure and urban activity, we used data from OpenStreetMap (OSM), a crowd-sourced digital map of the world. But instead of using just the current OSM data (which only reflects the present), we also needed historical versions for each year.

How We Collected OSM Data:

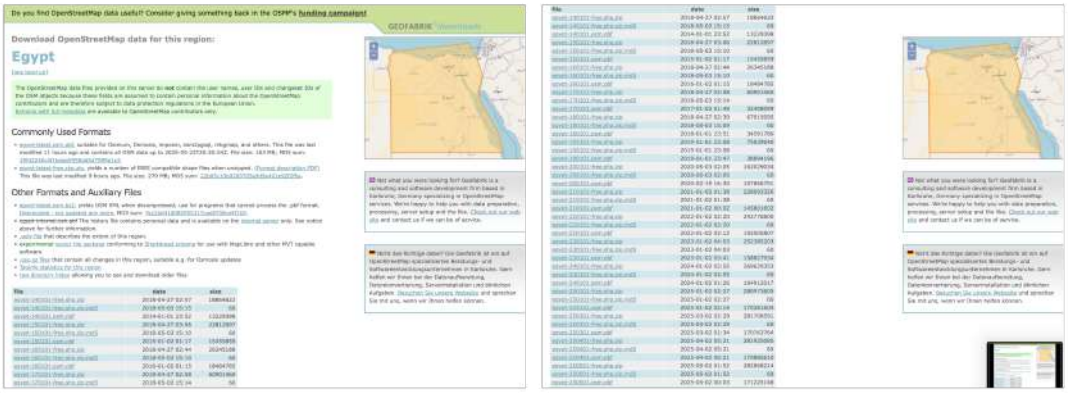

Figure 3.4: OSM Data Collection Steps

- We downloaded past OSM data from the Geofabrik Raw Directory Index (https://download.geofabrik.de)
- From this, we extracted:
  - **Points of Interest (POIs):** Locations such as stores, schools, hospitals, or gas stations.
  - **Roads:** All street and highway lines.
- Downloaded Egypt shapefiles for the years 2019, 2020, 2022, 2024, and 2025
- Each download included multiple layers such as:

  - gis_osm_pois_free_1.shp (Points of Interest)
  - gis_osm_roads_free_1.shp (Roads)
- Using GIS software (ArcGIS Pro), these files were then:
  - Clipped to Cairo using a shapefile
  - Projected to match Landsat's UTM coordinate system

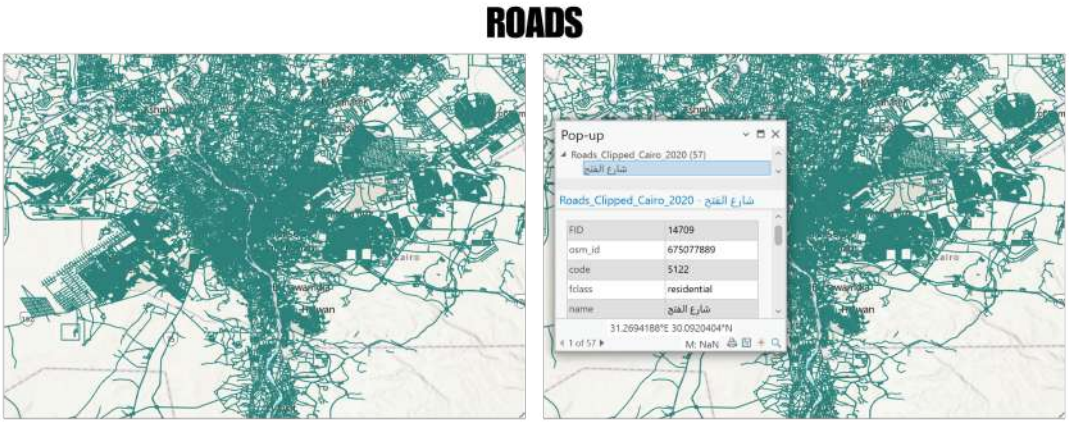

Figure 3.5: Roads Shapefile Sample

- We processed these layers to generate:
  - **Kernel Density maps of POIs:** Showing the concentration of important locations in each part of the city.
  - **Line Density maps of roads:** Indicating how dense the road network is in different areas.

This allowed us to approximate the functional intensity of each neighborhood based on its physical layout and services.

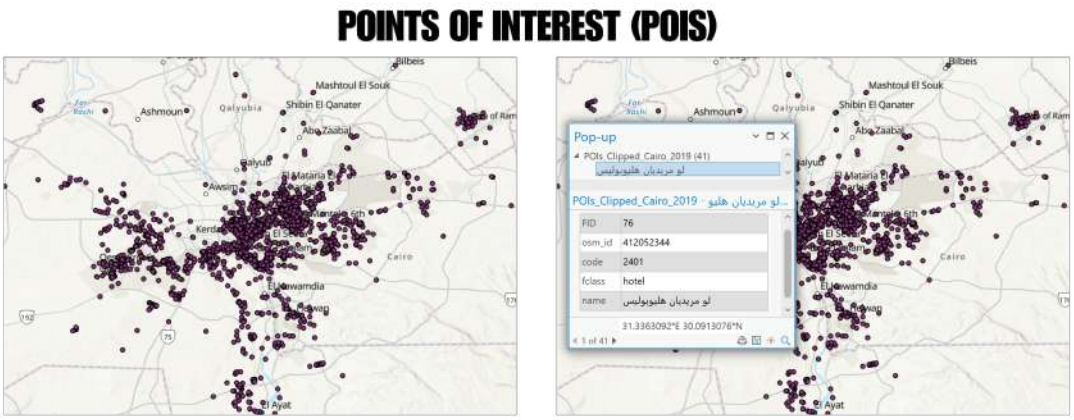

Figure 3.6: Points of Interest Shapefile Sample

3.0.4 VIIRS Nighttime Lights Data (Target Variable)

The most critical dataset was the **VIIRS nighttime lights imagery**, which captures how brightly different parts of the Earth glow at night. Brighter areas typically mean more electricity, businesses, and infrastructure, making it a good proxy for local economic development.

We used data from the **Visible Infrared Imaging Radiometer Suite (VIIRS)**, which is available for free from NASA's data servers. Specifically, we used the product called:

> **"vcm-cfg average masked monthly radiance"**

This means:

- **"Average masked":** It averages all the cloud-free nights in a month, removing moonlight, cloud, and fire noise.
- **"Radiance":** It gives the actual light intensity in a scientific unit: $\mu W/cm^2/sr$.
- **"VCM-CFG":** It's the cleaned, corrected, and filtered version of the raw VIIRS lights.

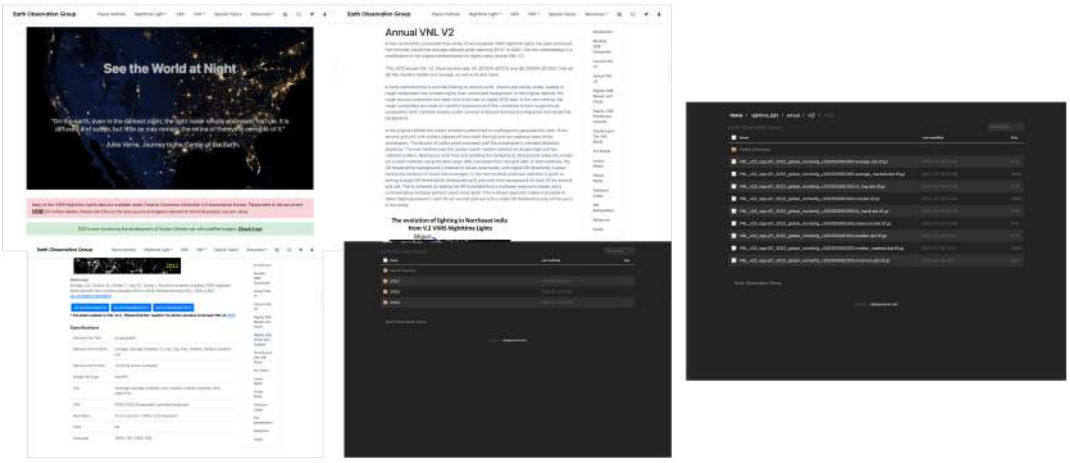

Figure 3.7: VIIRS Data Collection Steps

After downloading the files, we:

1. **Clipped** the VIIRS image to match the Cairo boundary.
2. **Reprojected** it to the same UTM coordinate system.
3. **Resampled** it to match the resolution of the Landsat images (30 meters per pixel).

When we say that an image has a resolution of **30 meters per pixel**, it means that **each individual pixel in the image represents an area of 30 meters by 30 meters on the ground**. In other words, **one pixel is equivalent to 900 square meters** of land area.

This spatial resolution is typical of **Landsat imagery**, which is designed to balance detail with broad coverage. At this resolution, we can capture urban patterns, agricultural areas, and infrastructure changes, but we cannot resolve small objects like individual cars or people.

In this project, we **resampled** other data sources (e.g., the VIIRS Nighttime Lights) to this 30m resolution to ensure consistency across all raster inputs, allowing pixel-by-pixel

alignment and meaningful model training.

These processed VIIRS images became our **ground truth**, the actual economic brightness levels that we trained our model to predict. Our ultimate goal was to use the Landsat images (which are available even in present years) to estimate what the VIIRS brightness is in **2025**, a year for which nighttime imagery is not yet released.

3.0.5 Shapefiles for Map Boundaries and Overlays

Throughout the project, we used multiple **shapefiles**, which are geographic data files that define the **shape and outline of a region**, in our case, the city of Cairo and its districts. These shapefiles were critical in:

- **Clipping** satellite images to focus only on our study area

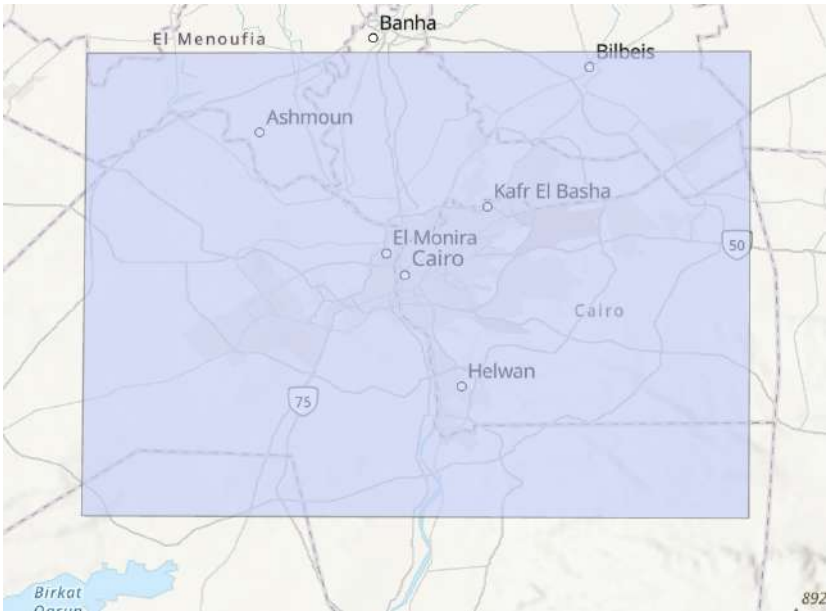

Figure 3.8: Area of Interest Shapefile

- **Ensuring spatial consistency** across all datasets
- **Overlaying boundaries** on top of our final predicted maps to show meaningful administrative regions, such as districts, neighborhoods, and landmarks

The shapefiles were used both in preprocessing (to extract only the relevant parts of

Figure 3.9: Boundaries and District Names Shapefile

each image) and in **final visualization**, allowing us to connect abstract predictions to real-world places that stakeholders and readers could recognize by overlaying city boundaries and district names on final maps.

Chapter 4

Methodology

4.0.1 Overview of the Methodological Pipeline

The goal of this project was to build a system that could **predict economic development**, measured as **nighttime brightness**, using **daytime satellite images and urban infrastructure data**.

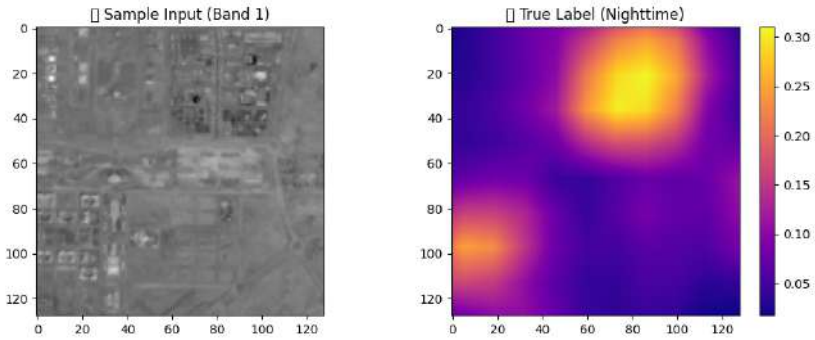

Figure 4.1: Sample Input (Band 1) Vs. True Label (Nighttime)

To achieve this, we followed a clear and repeatable pipeline consisting of the following stages:

Step 1: Data Collection

We downloaded and organized the following raw data:

- Landsat 8/9 daytime satellite images (7 bands per year) from USGS EarthExplorer
- VIIRS nighttime light data (1 image per year) from NASA's VIIRS product archives

- OpenStreetMap (OSM) files for roads and points of interest (POIs) from Geofabrik's historical shapefile archive
- Boundary shapefiles for Cairo from administrative GIS sources

Each file was placed into a structured folder system, grouped by region (Cairo) and year (e.g., 2018–2025).

Step 2: Preprocessing the Raw Data in ArcGIS Pro

Using **ArcGIS Pro**, we processed the satellite and map data through the following steps:

- **Mosaicking** Landsat tiles to cover full Cairo
- **Clipping** all rasters and vector layers to the exact Cairo boundary
- **Setting consistent NoData values** to -9999 for all layers
- **Projecting** everything to a unified coordinate system: WGS 1984 / UTM Zone 36N
- **Calculating indices** like NDVI, NDWI, and NDBI
- **Creating density maps** for POIs and roads
- **Exporting final composite images** and nighttime lights rasters per year

This gave us clean, spatially consistent datasets, year by year.

Step 3: Composite Construction

We then **stacked all the useful layers** together to form a "composite" image for each year. Each composite contained:

- 7 Landsat bands
- 3 spectral indices (NDVI, NDWI, NDBI)
- 2 infrastructure density maps (POIs and roads)

So, **each pixel** in the composite had **12 values** describing it.

Step 4: Model Training (2021)

We trained a deep learning model called **DeepLabV3+** using the 2021 composite (input) and VIIRS brightness values (target). The model learned how different combinations of features (like roads, vegetation, buildings) are related to economic brightness

at night.

Step 5: Model Testing and Prediction

Once trained, the model was tested on multiple years (e.g., 2018, 2019, etc.) to evaluate how well it performs. Then, it was used to **predict 2025 brightness**, where no VIIRS data exists yet.

Step 6: Evaluation and Visualization

We compared predicted maps to real VIIRS data using:

- Standard metrics (MAE, RMSE, R^2)
- Maps of residuals (errors)
- Scatter plots and heatmaps
- Visual overlays with Cairo's districts using shapefiles

This entire process was repeated for each year, allowing us to **visually and quantitatively assess economic change over time** and make future projections with confidence.

4.0.2 Data Preprocessing in ArcGIS Pro

Before we could use the satellite images and map layers to train a machine learning model, we first had to **clean, align, and prepare all of the data** so that it was consistent across space and time. This step was crucial, **any mistake here would lead to inaccurate model predictions** or invalid analysis. We used **ArcGIS Pro**, a professional Geographic Information System (GIS) software, to carry out all preprocessing steps.

GIS software works with data that is tied to real-world locations. ArcGIS Pro allowed us to visualize, manipulate, and process all the spatial files, both raster images (like satellite imagery) and vector files (like roads and city boundaries), in a spatially accurate and consistent way.

Below is a breakdown of each process and its purpose.

Organizing the Data

All data files were placed into a carefully structured folder system grouped by:

- **Region:** Cairo (other cities or regions could be added in the future)

- **Year:** 2018, 2020, 2021, 2022, etc.
- **Data type:**
  - **Landsat** for daytime satellite imagery
  - **VIIRS** for nighttime brightness
  - **OSM** for infrastructure and human activity data
  - **Indices** for calculated vegetation, water, and urban maps
  - **Densities** for road and POI concentration maps
  - **Composites** for the final stacked raster used by the model

Why this matters: Keeping everything organized ensured the process could scale to multiple years without confusion. It also made the pipeline easy to replicate or reuse.

Mosaicking: Combining Image Tiles

Landsat satellite images are not captured as one large image of a city. Instead, they come in **tiles**, each one a rectangular section of Earth captured during the satellite's pass. Cairo, for instance, is typically split across **two adjacent tiles**, due to its spatial extent and the way Landsat orbits the Earth.

Each tile contains all seven spectral bands for that year (e.g., Band 4 for red light, Band 5 for near-infrared), but only covers part of the target area. To analyze the entire city as a unified dataset, we first needed to **merge these adjacent tiles into one continuous raster**.

For each year:

- We downloaded both tiles for Cairo from **USGS EarthExplorer**
- For each spectral band, we used ArcGIS Pro's **Mosaic To New Raster** tool to combine the two tiles into one seamless image

How mosaicking works: When the tiles overlap, especially at the borders, the same geographic area may appear in both rasters with slightly different reflectance values due to differences in lighting, atmospheric conditions, or acquisition times. To resolve these overlaps:

- We applied the **Mean** mosaic operator, which computes the average of overlapping pixel values from both tiles.

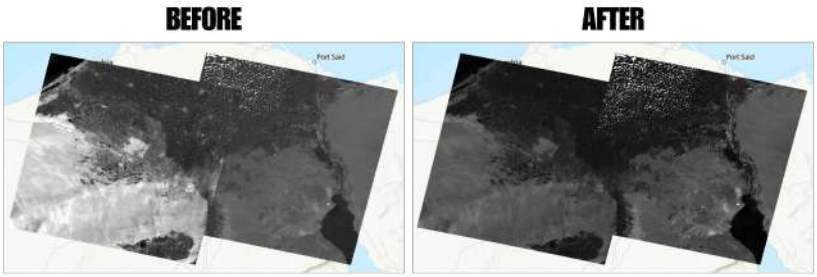

Figure 4.2: Band 1 Before and After Mosaicing

- This helps reduce abrupt transitions or seams between tiles and ensures a more visually and numerically consistent mosaic.

The output mosaic maintains the original Landsat spatial resolution of **30 meters per pixel**, meaning each pixel in the final raster represents a 30m × 30m area on the ground. This resolution is preserved during mosaicking, ensuring consistent spatial detail across the full image.

Why this matters: Machine learning models can't learn from incomplete data. We needed full coverage of the city so that every neighborhood, from central Cairo to the outer edges, was included in both the inputs and the predictions. Mosaicking must be done band by band, because Landsat delivers each spectral band as a separate file.

Clipping: Focusing Only on Cairo

After mosaicking, our images still included parts of Egypt outside Cairo, such as desert areas or nearby towns. These were not part of our study. So, we used a **shapefile**, a common GIS file format that defines the **geographic boundary of a region**, to cut out just the area of Cairo.

In ArcGIS Pro:

- We used the **Clip tool**
- The input was the full raster image or vector file

- The clip boundary was our **Cairo shapefile**

We clipped:

- All 7 Landsat bands
- Each VIIRS nighttime image
- Spectral indices (NDVI, NDWI, NDBI)
- Road and POI shapefiles (to remove features outside the city)
- Density raster outputs

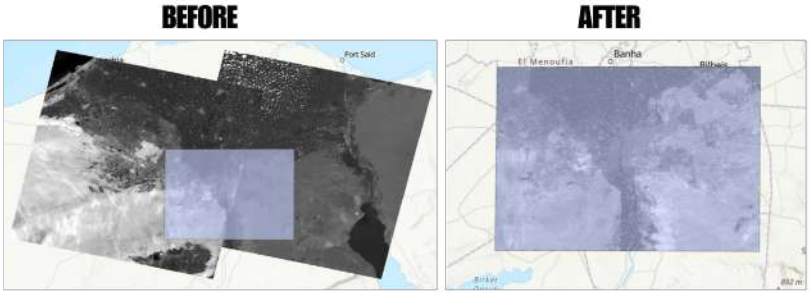

Figure 4.3: Band 1 Before and After Clipping

Why this matters: Clipping ensures the model only learns from data that actually belongs to the study area. Otherwise, the model might get confused by patterns that don't apply to Cairo. Shapefiles (.shp) also include metadata and projection info, which help define the exact shape and position of the region.

Setting NoData Values

Raster images (satellite layers) contain grids of pixels, each holding a numeric value. But not all pixels are valid:

- Some are **blank** (outside the clipped boundary)
- Others are **corrupted or cloud-covered**
- Some come from overlapping tiles and don't align well

We handled this by:

- Assigning **-9999** as a special "NoData" value
- Using ArcGIS Pro's **Set Raster Properties** tool

Later, in Python, we made sure our code **automatically ignores -9999 values** during training, evaluation, and prediction.

Why this matters: If the model sees garbage data (e.g., a blank pixel where a neighborhood should be), it will learn false patterns. This causes poor performance and bad predictions. NoData masking is especially important for deep learning, where every pixel contributes to the model's understanding.

Reprojecting: Aligning All Maps

Different satellite and map sources use different "projections", mathematical formulas for turning Earth's curved surface into a flat map. If not corrected, **pixels from different layers won't line up properly**, even if they're from the same location.

We used:

- **Project Raster** for raster data (e.g., Landsat, VIIRS)
- **Project** for vector data (e.g., roads, shapefiles)

All layers were converted to **WGS 1984 UTM Zone 36N**, which is:

- Accurate for Egypt
- Compatible with distance-based calculations (like densities)
- Widely supported in GIS and remote sensing applications

Why this matters: Misaligned layers = wrong inputs. Imagine if the brightness data was a few pixels off from the buildings map, it would completely mislead the model.

Calculating Spectral Indices (NDVI, NDWI, NDBI)

These are **mathematical formulas** used to extract more meaningful information from the raw bands. In ArcGIS Pro, we used the **Raster Calculator** with safe expressions:

- **NDVI (vegetation):**

  (Band 5 – Band 4) / (Band 5 + Band 4)

- **NDWI (water presence):**

(Band 3 – Band 5) / (Band 3 + Band 5)

- **NDBI (built-up areas):**

  (Band 6 – Band 5) / (Band 6 + Band 5)

Each formula was wrapped with a `Con()` condition to avoid dividing by zero, and output rasters were saved with NoData = -9999.

3.3

Why this matters: These indices summarize patterns (e.g., green parks, rivers, concrete zones) that aren't easily visible in the raw data, but are vital for understanding economic differences between areas.

Processing OSM Data: Densities from Roads and POIs

We used **OpenStreetMap shapefiles** downloaded from **Geofabrik's raw directory**, which offers historic snapshots of map data by year. From each year's folder, we extracted:

- `gis_osm_pois_free_1.shp`: points of interest (POIs) like schools, clinics, markets, etc.
- `gis_osm_roads_free_1.shp`: street and road networks

To convert these vector shapefiles into useful raster layers aligned with our satellite imagery, we:

- **Clipped** each shapefile to Cairo's official boundary to isolate the area of interest
- **Reprojected** all vector data to the UTM Zone 36N coordinate system to ensure consistent units (in meters) across all calculations
- Applied **Kernel Density** on the POI shapefiles: this tool calculates the density of points (e.g., number of clinics or schools) around each cell in the output raster (500m search radius)
  - A **500-meter search radius** means that for each pixel, the tool looks in a 500-meter circular neighborhood around it and counts nearby POIs
  - The result is a smooth, continuous raster showing how densely POIs are distributed across the city
- Applied **Line Density** on the road shapefiles: this calculates the total length of roads within a 500-meter radius of each pixel

  - This produces a raster where higher values represent areas with denser road networks (e.g., urban centers)

- Saved the resulting rasters in `.img` format to preserve data integrity and metadata
- Explicitly set the NoData value to **-9999** to ensure compatibility with other raster layers and avoid invalid values during model training

These density maps are crucial for modeling urban structure, as they capture the spatial footprint of human activity and infrastructure beyond what is visible in satellite imagery alone.

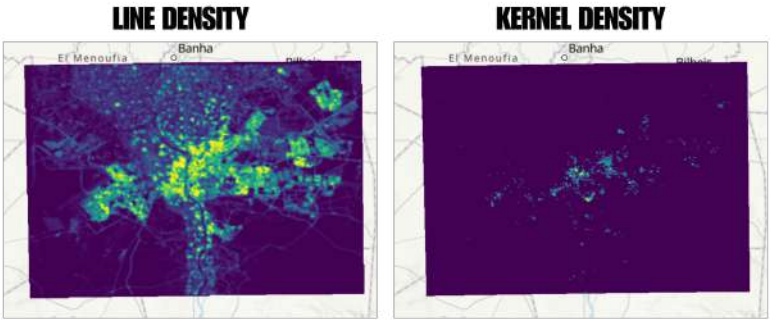

Figure 4.4: Densities Sample

Why this matters: Dense road networks and clusters of POIs are strong indicators of economic activity and accessibility. These maps added vital "urban structure" features to our model. Unlike satellite imagery, OSM is human-drawn but offers excellent insight into infrastructure.

Processing VIIRS Nighttime Lights

We downloaded VIIRS monthly images in `.tif` format from NASA. These measure how much light is detected from each area at night, bright cities glow, while rural areas are dark.

We chose:

- **"VCM-CFG average masked radiance"** product:

- Cloud-free and corrected

We:

- **Clipped** the VIIRS raster to Cairo's boundary
- **Reprojected** it to UTM Zone 36N
- **Resampled** it to 30m resolution (to match Landsat)
- Set **NoData to -9999**

Why this matters: This is the target that the model tries to predict. If this data is incorrect or unaligned, the model's learning will be useless.

Final Composite Generation

Once all components were ready, we built a **final multi-band raster** for each year. This composite included:

- 7 Landsat bands
- 3 indices (NDVI, NDWI, NDBI)
- 2 OSM-based density maps

In total, each pixel had **12 values** representing its appearance, function, and context.

We used:

- **Composite Bands** tool to stack them
- **Set Raster Properties** to re-apply NoData = -9999
- Final **visual checks** in ArcGIS Pro to confirm perfect layer alignment

Why this matters: This composite was the input to the model. Each pixel's "profile" told the model everything it needed to predict development brightness.

4.0.3 Composite Image Construction

Once all the individual satellite layers, indices, and urban density maps were preprocessed, cleaned, and aligned in ArcGIS Pro, the next critical step was to **combine them into a single, unified dataset** for each year. This combined file is called a **composite raster**, and it acts as the **"input image"** for the machine learning model. Just like a regular image has three channels (red, green, blue), our composite image had **12 channels**, each carrying a specific piece of information about the land.

Each pixel in the composite image represented a real-world location in Cairo, and the **12 values** attached to that pixel described everything we knew about that spot, from the color of its surface to how many roads or schools were nearby. Below is a step-by-step explanation of how the composite images were constructed and why this process is so important.

What is a composite raster, and Why Is It Needed?

A **composite raster** is a single file that stacks multiple input layers, called "bands", into one dataset. Each band contains a different type of information, and together, they form a rich, multi-dimensional view of the land.

Think of it like this:

Each composite raster is like a 12-layer cake. Each layer (or band) contributes a different flavor:

- Some layers represent natural features (e.g., vegetation)
- Others represent human-made features (e.g., roads)
- All layers are aligned so that each "slice" (pixel) contains a full stack of data for that specific location

This is the format that our machine learning model expects. Just like a facial recognition AI needs RGB pixel data to identify a face, our model needs 12-band composite pixel data to identify economic development patterns.

Selecting the 12 Input Layers

For each year (e.g., 2018, 2021, 2023), we selected **exactly 12 raster layers** to include in the final composite:

Landsat Bands (7 layers):

1. **Band 1 – Coastal (atmospheric correction)**
2. **Band 2 – Blue**
3. **Band 3 – Green**
4. **Band 4 – Red**
5. **Band 5 – Near Infrared (vegetation)**
6. **Band 6 – Shortwave Infrared 1 (built-up detection)**

7. **Band 7 – Shortwave Infrared 2 (thermal/moisture)**

??

These bands reflect how light interacts with different surfaces (e.g., asphalt, grass, concrete, water). Each band focuses on a different wavelength and helps capture the physical properties of the surface.

Spectral Indices (3 layers):

1. **NDVI (Normalized Difference Vegetation Index)**

   Measures how green an area is.

2. **NDWI (Normalized Difference Water Index)**

   Detects presence of water.

3. **NDBI (Normalized Difference Built-up Index)**

   Identifies urban structures.

3.3

These were computed directly in ArcGIS Pro using the Raster Calculator and ensure that the model gets a clearer understanding of land use.

Infrastructure Density Maps (2 layers):

1. **Kernel Density of Points of Interest (POIs)**

   Highlights how many services and facilities are nearby (e.g., schools, clinics).

2. **Line Density of Roads**

   Indicates how dense and accessible the street network is.

These two layers were derived from OSM data and reflect **human activity and connectivity**, which are essential for predicting economic development.

4.4

Preparing the Layers for Merging

Before combining the layers into a composite, we ensured the following:

- All rasters were **projected to the same coordinate system** (WGS 1984 UTM Zone 36N)

- All rasters had **the exact same pixel dimensions**, extent, and resolution (30 meters per pixel)
- All layers had **NoData values set to -9999**
- Each file was visually checked in ArcGIS Pro to confirm that all layers perfectly overlapped (i.e., no misalignment)

This step is vital. If even one layer had a different shape or coordinate system, the composite would fail, or worse, silently produce misaligned data, which would corrupt the model's learning process.

Creating the Composite Raster

To create the composite, we used the **"Composite Bands"** tool in ArcGIS Pro. This tool takes multiple input rasters and stacks them into one multi-band file.

Steps followed:

1. Selected the 12 input layers for a given year
2. Verified that all had the same extent and pixel size
3. Ran the Composite Bands tool
4. Saved the output to a new folder named **Final_Composites**
5. Manually verified the resulting file using **Layer Properties ¿ Bands** to ensure all 12 bands were present and correctly ordered

Each composite raster was named in the format:

`Composite_Cairo_<Year>_cleaned.tif`

For example:

- `Composite_Cairo_2021_cleaned.tif`
- `Composite_Cairo_2025_cleaned.tif`

What this file contains:

For every 30m x 30m pixel in Cairo, this TIFF file stores:

- The surface reflectance in 7 light bands
- Vegetation, water, and built-up scores

- Local infrastructure intensity

Final Quality Check and NoData Fix

Even after stacking, a few artifacts or inconsistencies may remain. So we applied a **final raster cleaning step**:

- Used the **Copy Raster** tool to re-encode NoData = -9999 at the composite level
- Deleted the temporary version
- Renamed the fixed copy back to its original name

Then, for each composite:

- We opened it in ArcGIS Pro
- Overlaid it with the Cairo shapefile boundary
- Verified that all features were properly visible, sharp, and well-aligned

Why Composite Construction Is So Important

Machine learning models don't "see" like humans, they rely on numbers. Every composite we constructed served as a **numerical fingerprint of Cairo for a specific year**. Without these stacked, multi-layered inputs, the model would be blind to the complex interactions between:

- Natural land features (vegetation, water, bare soil)
- Urban infrastructure (buildings, roads)
- Human activity intensity (services, transport networks)

Only when these layers are **combined into one image**, pixel by pixel, can a model be trained to learn what economic development "looks like" from above.

4.0.4 Training the Model (2021 Data)

After building the model architecture (DeepLabV3+) and preparing our composite input images, we reached the heart of the project: **training the model**. Training is the process where the model **learns patterns from past data** so that it can make accurate predictions on new, unseen data. Our model learns by looking at known examples from **2021**, where we already have both:

- The input features (composite image with 12 layers), and
- The label (the true VIIRS brightness values)

This section explains **how we trained the model using 2021 data**, including how the data was formatted, split, processed, and passed through the model.

What Does Training a Model Mean?

In simple terms, training means:

1. Showing the model an image of a small area (e.g., a 128×128 pixel tile of Cairo)
2. Letting it **guess** how bright each part of that area is at night
3. Comparing its guesses to the **actual VIIRS brightness**
4. Measuring how wrong it was
5. Making **tiny adjustments** to the model so it gets a bit better
6. Repeating this process **thousands of times**

Over time, the model gets smarter. It starts noticing patterns and associations, like "dense roads usually mean more lights" or "green fields are usually darker."

Preparing the Data for Training

Raw images are too large to be passed into the model all at once, so we **split the 2021 composite and VIIRS images into smaller square sections/tiles** to make training efficient and scalable.

Step-by-step:

- Input image: `Composite_Cairo_Train_2021_cleaned.tif`
- Label (target): `VNL_Cairo_2021_Final.tif`
- Using a sliding window approach:
  - **Tile size:** 128×128 pixels (represents a small neighborhood)
  - **Stride:** 64 pixels (controls overlap between tiles)
- Skipped any tiles that had **missing (NoData = -9999)** values in any of the bands or label

The result:

A large dataset of matching input and output tile pairs, where each pair:

- Input: A 128×128×12 array (12 layers per pixel)
- Label: A 128×128 array of brightness values (one value per pixel)

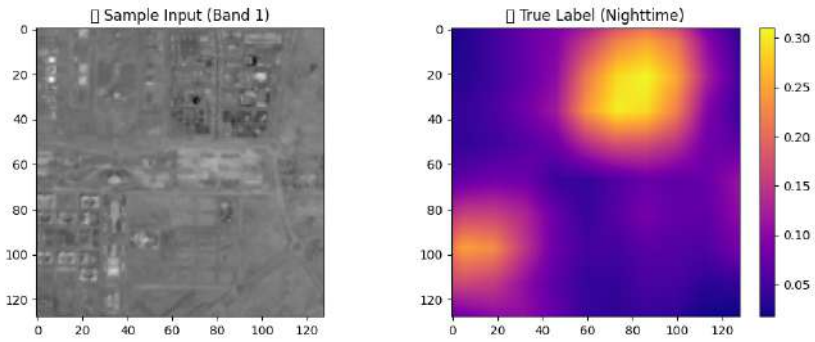

Figure 4.5: Sample Input and Label

Splitting Into Training and Validation Sets

To make sure the model is not just memorizing the data, we split the tile dataset into:

- **80% training tiles:** These were used to teach the model
- **20% validation tiles:** These were used to **test the model during training** to see how well it generalizes

This step is crucial to detect **overfitting**, which happens when a model performs well on the data it was trained on but fails on new data.

Feeding the Data into the Model

Once the tiles were ready, we converted them into tensors, structured numeric arrays that deep learning frameworks like PyTorch can understand.

We used:

- `TensorDataset|` to store training and validation data
- `DataLoader|` to:
  - Feed the data to the model in **batches** (groups of 8 tiles at a time)
  - **Shuffle** the data to reduce bias
  - Enable automatic batching on GPU (faster training)

The input and label tensors were reshaped into the format:

- **Inputs:** `[batch_size, 12, 128, 128]`
- **Labels:** `[batch_size, 128, 128]`

Loss Function: Measuring How Wrong the Model Is

We used **Mean Squared Error (MSE)** as our loss function. It calculates the average squared difference between the model's predicted brightness and the actual VIIRS brightness.

$$\text{MSE} = \frac{1}{N}\sum_{i=1}^{N}(\text{prediction}_i - \text{actual}_i)^2$$

- **Lower MSE = better performance**
- Squaring the error gives more weight to large mistakes

We chose MSE because:

- It's standard for regression tasks
- It's sensitive to big errors
- It's simple to interpret and optimize

Optimizer and Learning Rate

We used the **Adam optimizer**, which is a smart algorithm that:

- Automatically adjusts how fast the model learns
- Helps the model avoid getting stuck in bad solutions

We set:

Learning rate = 0.0001

(This controls how big each model update is, small values lead to slower but more stable learning)

Training Loop (30 Epochs)

An **epoch** is one full pass through the entire training dataset. We trained the model for **30 epochs**, which means it saw each tile 30 times with slightly updated parameters each time.

In each epoch:

1. **Training Phase:**
    - The model predicted outputs on each training tile
    - We calculated the MSE loss
    - The optimizer updated the model weights
2. **Validation Phase:**
    - The model made predictions on the validation set
    - We recorded the validation loss without updating the weights
    - This helped track performance on unseen data

We plotted both training and validation loss over time to make sure the model:

- Was learning (loss decreasing)
- Was not overfitting (validation loss stays low)

Training Results

- Final training loss: **24.49**
- Final validation loss: **40.13**
- The gap between training and validation loss was small, indicating **good generalization**
- Visual inspection showed that predictions were structurally aligned with actual VIIRS maps

These results confirmed that the model had successfully **learned the relationship between satellite features and nighttime brightness**, at the pixel level.

Saving the Trained Model

After training, we saved the model's parameters to a file:

```
torch.save(model.state_dict(),"DeepLabV3Plus_Cairo2021_Weights.pth")
```

This allowed us to:

- Reuse the trained model without retraining

- Apply it to new years (2018–2025)
- Safely continue work after restarting the environment

4.0.5 Prediction & Evaluation Process

After training our DeepLabV3+ model using 2021 data, we moved on to the final phase: **testing the model** on other years and **evaluating how well it performed**. This stage served two goals:

1. **Prediction:** Apply the trained model to years it had never seen (like 2018 or 2023) to generate new economic development maps.
2. **Evaluation:** Compare the model's predictions to actual nighttime brightness data from VIIRS to measure accuracy.

This section explains the full process of how we used the model, what metrics we used to evaluate performance, and how we visualized and interpreted the results.

Making Predictions on New Years

With the model trained on Cairo 2021, we now applied it to new data from other years:

- Past: 2019, 2020, 2022, 2023, and 2024
- Present/Future: 2025 (no VIIRS available)

How Prediction Works: We loaded the trained model using:

```
model.load_state_dict(torch.load("DeepLabV3Plus_Cairo2021_Weights.pth")) model.eval(
```

1. We took each year's composite raster (e.g., `Composite_Cairo_2023_Test_cleaned.tif`) as the input.
2. The raster was divided into **overlapping tiles (128×128 pixels)** just like in training.
3. For each tile, the model predicted nighttime brightness values for all pixels.
4. The predictions were **stitched back together** into one large output raster, our **Predicted Economic Development Map**.

This output had the same spatial resolution (30 meters per pixel) and the same dimensions as the VIIRS ground truth data.

Each output file was saved as a GeoTIFF, for example:

- `Predicted_Dev_Map_DeepLab_Cairo_2023.tif`
- `Predicted_Dev_Map_DeepLab_Cairo_2025.tif`

Comparing Predictions to Ground Truth

For years where VIIRS data was available (2019–2024), we compared:

- **Actual map:** VIIRS image (real measured brightness)
- **Predicted map:** Our model's output

To do this, we:

- Made sure both maps were aligned pixel-for-pixel
- Ignored any NoData values
- Focused only on valid areas inside Cairo

This comparison allowed us to **quantitatively assess how accurate our predictions were**, and **visually see how close they looked**.

Evaluation Metrics

We used three well-known statistical metrics to evaluate the performance of the model:

1. Mean Absolute Error (MAE) This tells us, on average, how far off the model's prediction was from the actual brightness:

$$\text{MAE} = \frac{1}{N} \sum_{i=1}^{N} |\text{Prediction}_i - \text{Actual}_i|$$

- Lower MAE = better accuracy
- Easy to interpret (e.g., "On average, we're off by 6 units of brightness")

2. Root Mean Squared Error (RMSE) This is like MAE, but it **penalizes bigger mistakes more heavily**:

$$\text{RMSE} = \sqrt{\frac{1}{N} \sum_{i=1}^{N} (\text{Prediction}_i - \text{Actual}_i)^2}$$

- More sensitive to outliers

- Used for understanding maximum deviation risk

3. R-squared (R^2) This tells us **how well the model explains the variation** in the data:

- $R^2 = 1.0$ means perfect prediction
- $R^2 = 0$ means random guessing

It shows how much of the economic brightness variation can be explained by the model's understanding of satellite and urban features.

Visual Evaluation: Maps, Scatter Plots, and Heatmaps

Numbers tell part of the story, but visualizing the results makes patterns more obvious and intuitive.

For each evaluated year, we created:

- **True VIIRS Map** (ground truth brightness)
- **Predicted Map** (model output)
- **Residual Map** (difference = actual – predicted)
- **Scatter Plot:** Actual vs Predicted (each pixel as a dot)
- **Histogram of Residuals:** Frequency of errors
- **Heatmap of Absolute Error:** Shows where the model struggled

These visuals helped confirm:

- Whether the model underestimated or overestimated brightness
- Which parts of the city were more difficult to predict
- How prediction quality changed over time

Example Results (Cairo 2023)

For 2023, the model achieved:

- **MAE:** 8.13
- **RMSE:** 11.31
- **R^2:** 0.8207

These results show **high accuracy**. The model correctly predicted economic patterns across most of Cairo, especially in bright, dense areas like downtown, new districts, and key corridors. Some underestimations occurred in areas with extreme brightness or rapid new development.

Mapping the Present/Future (Cairo 2025)

Unlike previous years, **no VIIRS image exists for 2025** so this prediction is the **true purpose of the model: to forecast unseen development**.

We:

- Input: `Composite_Cairo_2025_Prediction_cleaned.tif`
- Applied the same tile-by-tile process
- Generated: `Predicted_Dev_Map_DeepLab_Cairo_2025.tif`

The resulting map gives policymakers, planners, and researchers a **view of how Cairo's economic activity looks like**, based purely on infrastructure and land features visible from space.

Summary: Why This Matters

This final stage proved the value of our entire pipeline:

- We turned free satellite images and maps into actionable predictions.
- We measured performance not just with numbers but with maps and visuals.
- We demonstrated that a model trained on one year (2021) could **generalize across time**, making it powerful for forecasting future development or assessing past progress.

Most importantly, we showed that **a model can be trained to "see" economic activity from the sky**, without any census or financial reports, opening the door to high-resolution development monitoring in data-poor regions.

4.0.6 Results

This section presents the results of applying the DeepLabV3+ model, trained on Cairo's 2021 satellite composite, to predict economic development (as measured by VIIRS nighttime light intensity) for the years 2019, 2020, 2022, 2023, 2024, and 2025. The model outputs a continuous brightness map for each pixel, which we evaluated against ground-truth VIIRS maps wherever available.

Each evaluation included:

- Full-map predictions for the entire Cairo region
- Visual diagnostics (residuals, scatter plots, error heatmaps)
- Statistical performance metrics: MAE, RMSE, and R^2
- Error distribution analysis across brightness quantiles

Overview of Evaluation Metrics

The following table summarizes the performance metrics across all evaluated years. These were computed by flattening only valid (non-NoData) pixels in both the predicted and ground truth VIIRS images.

Year	MAE	RMSE	R^2
2019	9.20	18.89	0.5155
2020	9.25	16.69	0.5368
2022	6.78	14.08	0.7442
2023	8.13	11.31	0.8207
2024	6.68	12.98	0.7742

Table 4.1: Performance metrics for DeepLabV3+ predictions across years with available VIIRS data

Cairo 2023 — Peak Model Accuracy

The Cairo 2023 test results offer a comprehensive view into the spatial accuracy and limitations of the trained DeepLabV3+ model when applied to recent unseen data. Using the cleaned composite from 2023 as input and comparing the predicted development map to the actual VIIRS nightlight intensity, we evaluated model performance using multiple complementary techniques.

Quantitative Metrics

The core evaluation metrics for Cairo 2023 are as follows:

- **Mean Absolute Error (MAE) = 8.13**
- **Root Mean Squared Error (RMSE) = 11.31**
- **Coefficient of Determination (R^2) = 0.8207**

These metrics indicate strong overall performance. An MAE of 8.13 suggests that the model deviates from the true VIIRS value by an average of just over 8 brightness

units per pixel. RMSE is slightly higher due to its sensitivity to large outliers, but remains well within acceptable bounds. The R^2 score of 0.8207 implies that over 82% of the variation in nightlight intensity across Cairo is successfully explained by the model's predictions, which is notably high for pixel-wise regression from optical satellite imagery.

Visual Inspection and Spatial Agreement

Figure 4.6 (Top row) compares the actual 2023 VIIRS nightlight map to the predicted development map, followed by a residual map (True – Predicted). The predicted brightness distribution closely matches the ground truth, with the model successfully capturing:

- High-density urban clusters in **Nasr City, Heliopolis, Downtown Cairo, and Giza**
- Rapidly expanding zones such as **New Cairo 1, 2, and 3**
- Peripheral hotspots like **6th of October, Shaykh Zayed**, and parts of **Al Salam**

However, some limitations are visible:

- Slight overprediction occurs in rural transition areas south of Maadi and near Badr City.
- Local underpredictions are evident within dense industrial zones and ultra-bright urban centers (e.g., Tahrir Square, central Nasr City), where extreme brightness is often clipped or underestimated.

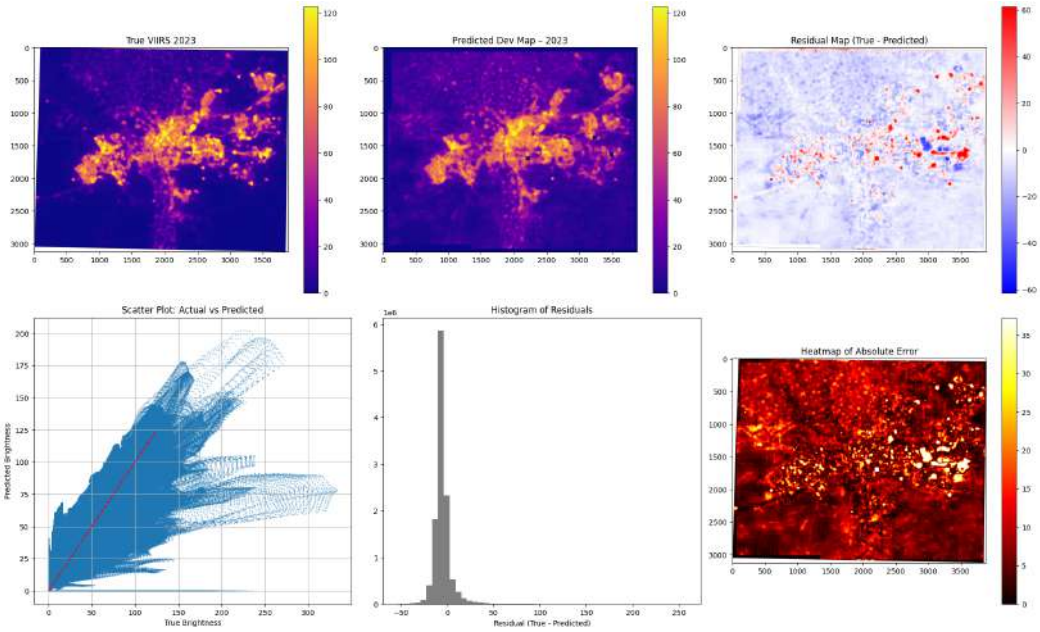

Figure 4.6: Top: True VIIRS 2023, Predicted Dev Map, and Residual Map. Bottom: Scatter Plot of True vs Predicted, Histogram of Residuals, and Absolute Error Heatmap.

Scatter Plot and Residual Distribution

The scatter plot (bottom-left in Figure 4.6) shows a strong linear relationship between predicted and actual brightness values. Most points cluster tightly around the 1:1 line, affirming prediction reliability. However, deviations become more pronounced for higher brightness levels above 150 units, where the model slightly saturates, a known issue in regression tasks involving skewed brightness distributions.

The residual histogram (bottom-center) displays a sharp peak near zero, confirming that most errors are minor. The distribution is slightly left-skewed, indicating a tendency toward mild overestimation in lower-brightness areas.

Spatial Error Patterns

The residual map and absolute error heatmap (top-right and bottom-right) reveal the geographic footprint of model discrepancies:

Errors are minimal in core urban neighborhoods with stable lighting patterns.

Elevated residuals cluster around **urban-rural edges**, newly constructed areas, and desert expansion zones, which are harder to learn from historic satellite data alone.

The absolute error heatmap visually highlights boundaries of under-served or rapidly

transforming regions where traditional indices may not fully capture socio-economic emergence.

District Overlay Validation

Figure 4.7 overlays predicted brightness onto Cairo's administrative boundaries. The model's output aligns remarkably well with district-level economic zoning:

- **Shubra, Nasr City, Heliopolis, and El Marg** show expected intensity peaks.
- Newly developed regions like **New Cairo and Shorouq** are correctly identified as rising economic hubs.
- Transitional zones such as **Al Tibbin, Badrashin, and Atfih** show lower predicted values, consistent with actual low-light observations.

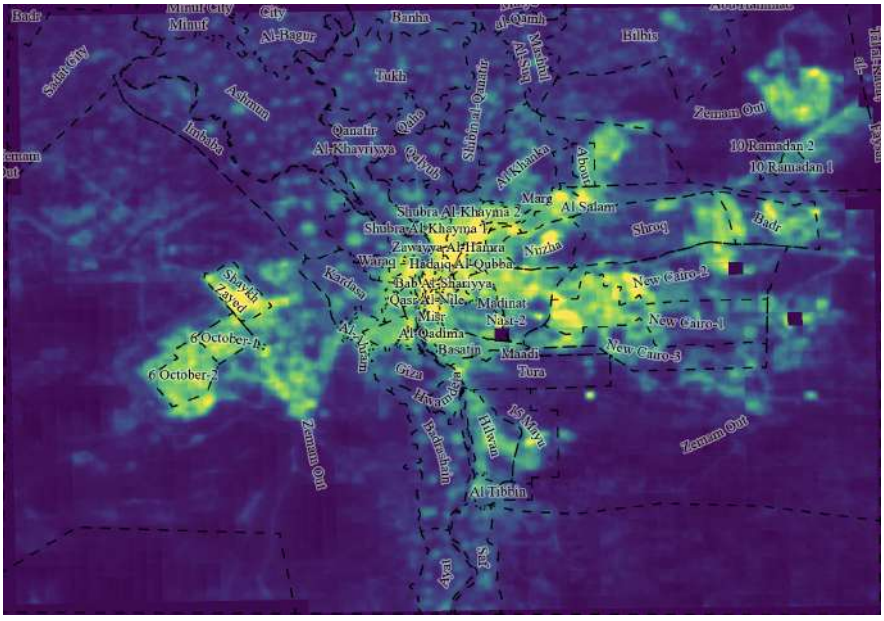

Figure 4.7: Overlay of Cairo District Map on Predicted Brightness (2023)

Conclusion

Cairo 2023 serves as a robust test case demonstrating the DeepLabV3+ model's ability to generalize across time. While high-brightness underestimation persists in some extreme cases, the overall spatial and statistical performance is strong. The model effectively captures both historical urban cores and newer expansion areas, providing a reliable basis for future prediction and policy insights.

Cairo 2024

The Cairo 2024 evaluation examines the model's ability to generalize forward in time and anticipate spatial economic patterns based solely on input features from satellite imagery. Despite the lack of real-time training data from this year, the model is tasked with forecasting development intensity that aligns with the actual VIIRS observations recorded in 2024.

Quantitative Metrics

The predictive performance of the model on Cairo 2024 is quantified as follows:

- **Mean Absolute Error (MAE) = 6.68**
- **Root Mean Squared Error (RMSE) = 12.98**
- **Coefficient of Determination (R^2) = 0.7742**

Compared to 2023, the MAE has improved, indicating smaller average pixel-level deviations. However, the RMSE has increased, signaling the presence of more extreme residuals. The R^2 score of 0.7742, while still strong, is slightly lower, meaning the model explains 77% of the variance in true 2024 brightness across Cairo.

Visual Inspection and Spatial Alignment

Figure 4.8 (Top row) displays the actual VIIRS nightlight intensity for 2024, the predicted development map, and the residual distribution (True – Predicted). Once again, the model accurately reconstructs major urban structures:

- Brightness is well captured in key hubs such as **Heliopolis, Nasr City, Giza, and Downtown Cairo**.
- Urban expansions into **New Cairo**, **Shorouq**, and **6th of October** are successfully highlighted.
- The emergence of light clusters in eastern suburbs, including **10th of Ramadan** and **Badr**, are partially detected.

Errors, however, increase in spatial complexity:

- A mix of underestimation and overestimation appears at the urban-rural interface.
- Noise or high variability is seen in some new developments where land cover signatures may not be distinctive yet in the input raster.

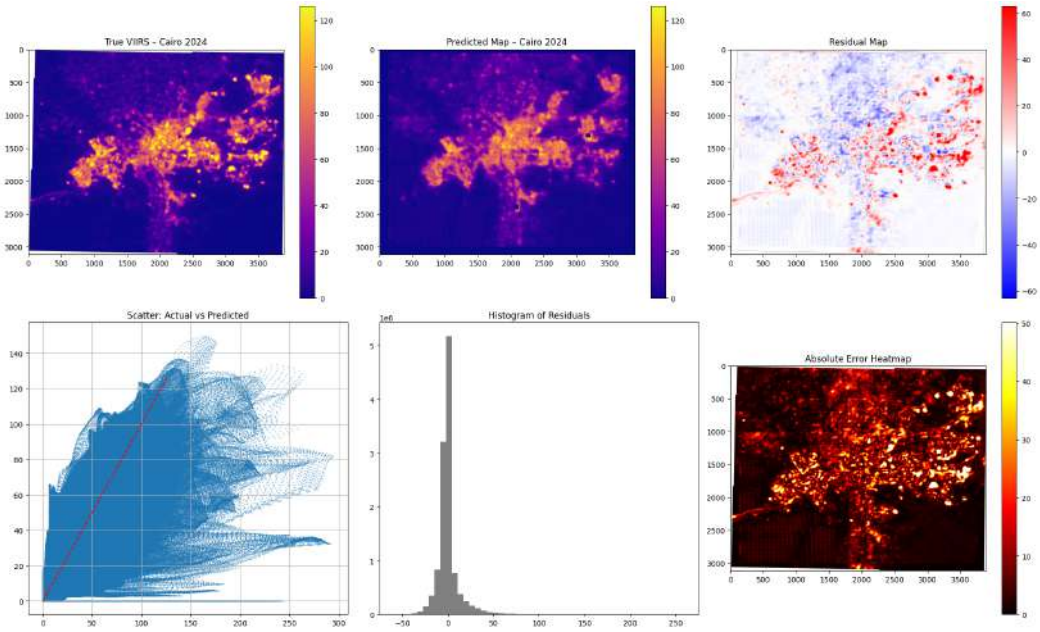

Figure 4.8: Top: True VIIRS 2024, Predicted Map, and Residuals. Bottom: Actual vs Predicted Scatter Plot, Histogram of Residuals, and Heatmap of Absolute Error.

Scatter and Residual Analysis

The scatter plot (bottom-left of Figure 4.8) confirms a linear correlation between true and predicted values, but the upper range (¿100 brightness units) shows broader dispersion than in 2023. This may be due to:

- Model smoothing effects that compress very high brightness values into midrange predictions.

The residual histogram shows a pronounced peak near 0, affirming that the majority of predictions are reasonably close. However, the longer right tail compared to 2023 suggests increased overprediction in some regions, possibly driven by aggressive learning from adjacent high-brightness zones.

Error Mapping and Interpretation

The residual and absolute error maps reveal that:

- Central Cairo and Giza remain highly stable with low residuals.

Error hotspots emerge in:

- **Al Salam and New Cairo districts**, due to partial overestimations

- Fringe areas east of **Badr** and south of **Maadi**, where spatial transitions confuse the model
- Sparse patches in **Shubra El-Kheima** and **Kirdasa**, where high building density may not align with training distribution

The absolute error heatmap confirms sharp spatial contrasts in predictive reliability, with urban cores exhibiting minimal error and expansion corridors reflecting higher model uncertainty.

District-Level Overlay Validation

Figure 4.9 shows the predicted 2024 map overlaid with Cairo's administrative boundaries. The predictions remain geographically coherent, with accurate delineation of:

- Dense urban centers such as **Heliopolis, Zamalek, and Nasr City**
- Rapid development corridors such as **New Cairo, 6th of October, and Shaykh Zayed**
- Lower-intensity zones like **Tura, Al Tibbin, and Atfih** matching actual VIIRS patterns

Figure 4.9: Cairo's Administrative Districts overlaid on Predicted Development Map (2024)

Conclusion

Despite being a forward-looking prediction, Cairo 2024 results affirm the model's strong temporal generalization capacity. While residual variance slightly increases compared to 2023, the model still retains a high degree of spatial accuracy and thematic fidelity. This reinforces its reliability as a forecasting tool for future economic development based on satellite-derived inputs.

Cairo 2022

The Cairo 2022 evaluation provides a mid-horizon snapshot of the model's predictive capability for a year closer to the training period but still unseen during training. This test helps assess whether the model's accuracy is consistent across recent years and whether it captures meaningful development signals in the 2022 landscape.

Quantitative Metrics

The performance on Cairo 2022 is summarized below:

- **Mean Absolute Error (MAE) = 6.78**
- **Root Mean Squared Error (RMSE) = 14.08**
- **Coefficient of Determination (R^2) = 0.7442**

The MAE remains low, indicating good average accuracy at the pixel level. However, the RMSE is the highest among all evaluated years thus far, pointing to the presence of larger outliers or occasional extreme deviations. The R^2 value of 0.7442 reflects a solid but slightly reduced ability to explain the spatial variation in brightness compared to 2023 and 2024, likely due to temporal mismatch or changes in urban morphology that the model could not fully anticipate.

Visual Comparison and Interpretation

Figure 4.10 (Top row) presents the true VIIRS nightlight intensity for 2022, the predicted development map, and the residual map (True – Predicted). The model exhibits strong alignment in key regions:

- Brightness hot zones like **Nasr City, Zamalek, Heliopolis, Downtown Cairo, and Giza** are predicted accurately.
- Peripheral development areas including **Shaykh Zayed, 6th of October, and New Cairo** appear with moderately strong predictions.

Despite accurate general shapes, several locations show mismatches in intensity or contour sharpness.

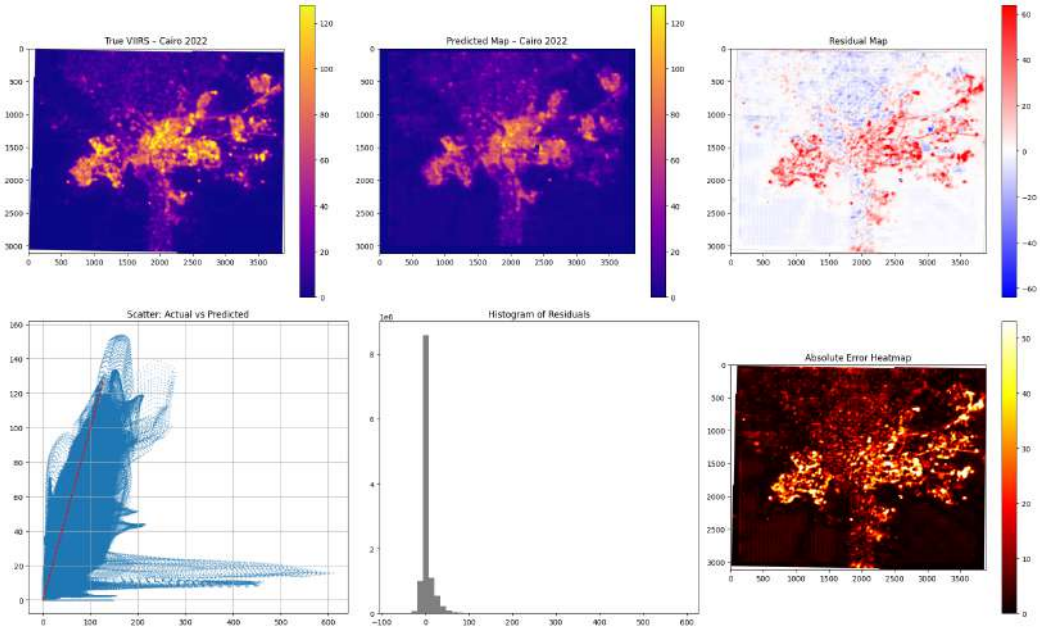

Figure 4.10: Top: VIIRS 2022, Model Prediction, and Residuals. Bottom: Scatter Plot of Actual vs Predicted, Residual Histogram, and Absolute Error Heatmap.

Scatter and Residual Analysis

The scatter plot (bottom-left) confirms a high concentration of points along the 1:1 line, especially in the low-to-mid brightness range. However, deviations increase substantially as brightness exceeds 100 units, with several predictions flattening out and underestimating extreme urban lights. This behavior contributes to the elevated RMSE score.

The histogram of residuals (center-bottom) is skewed slightly to the right, confirming that overestimation is more common in this year than underestimation. Additionally, the spread of residuals is wider than in 2023 and 2024, suggesting some inconsistency in model generalization over this particular snapshot.

Spatial Error Distribution

The residual and absolute error maps illustrate the nature of spatial discrepancies:

- Core metropolitan zones such as **Giza, Misr El-Qadima, and Downtown** retain high accuracy.
- Error intensifies in fringe areas undergoing dynamic change, notably:

- Southern and eastern edges such as **Maadi, 15 May City, and Badrashin**
- Emerging desert corridors leading to **New Cairo and Badr**

The absolute error heatmap (bottom-right) further emphasizes that while the center remains reliable, ring-like areas around the urban boundary exhibit greater prediction volatility, likely due to land use shifts, unaccounted informal expansion, or reflectance misclassification.

District Overlay Validation

Figure 4.11 overlays predicted development intensity on administrative boundaries for a spatial validation of performance. The following are confirmed:

- Brightness patterns tightly align with urbanized districts like **Nasr City, Heliopolis, and Shubra**.
- Development zones in **New Cairo, Al Salam, and 10th of Ramadan** are partially captured but with lower brightness than observed.
- Remote low-light regions such as **Zemam Out, Atfih, and Al Tibbin** remain correctly predicted as dark.

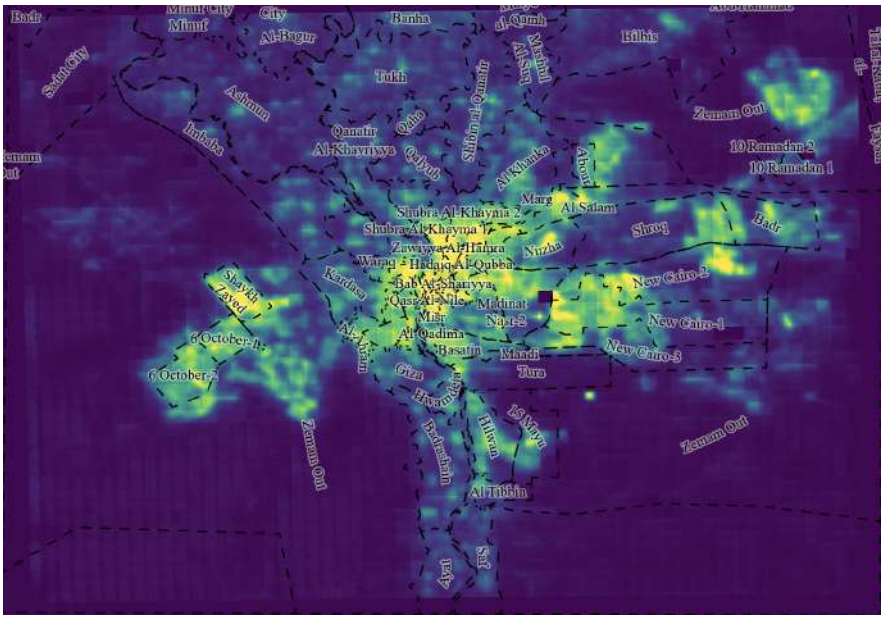

Figure 4.11: Predicted 2022 Development Map overlaid with Cairo District Boundaries

Conclusion

Cairo 2022 results demonstrate that the model continues to capture the overall urban morphology and brightness patterns with reasonable fidelity. However, it exhibits slightly reduced spatial precision compared to surrounding years, especially in peripheral and high-brightness areas. This outcome reflects the complex nature of urban change in transition years, underscoring the need for enhanced temporal features or retraining strategies for higher temporal stability.

Cairo 2020

The Cairo 2020 results offer an important insight into the model's temporal robustness when applied to data from three years prior to the 2023 test set and a full year before the 2021 training data. This makes 2020 a valuable backward test to assess model sensitivity to earlier development dynamics and potential generalization decay.

Quantitative Metrics

The model performance on Cairo 2020 is notably weaker than in surrounding years, with the following metrics:

- **Mean Absolute Error (MAE) = 9.25**
- **Root Mean Squared Error (RMSE) = 16.69**
- **Coefficient of Determination (R^2) = 0.5368**

An MAE of 9.25 reflects an increase in average pixel-level error compared to later years, and the RMSE of 16.69 suggests the presence of more pronounced outliers or extreme mispredictions. Most critically, the R^2 score drops to 0.5368, indicating that the model explains only about 54% of the variance in VIIRS brightness values, a significant decrease in explanatory power and spatial accuracy.

Visual Assessment and Discrepancy Patterns

Figure 4.12 shows clear limitations in the predicted map. While the core urban zones are still somewhat recognizable, the spatial sharpness and intensity gradients deviate more heavily from the true VIIRS observations. The model's predicted brightness appears flatter and smoother, failing to capture the high-luminance detail found in downtown Cairo, Nasr City, and Giza.

Several major observations arise:

- Underprediction dominates most of the map, especially in bright zones such as **Heliopolis, 6th of October, and Downtown**.
- Urban edges appear muted or overly smoothed, causing merged or missed clusters.
- Peripheral districts like **Al Tibbin, Badrashin, and Atfih** are somewhat well-predicted in shape but suffer from low intensity.

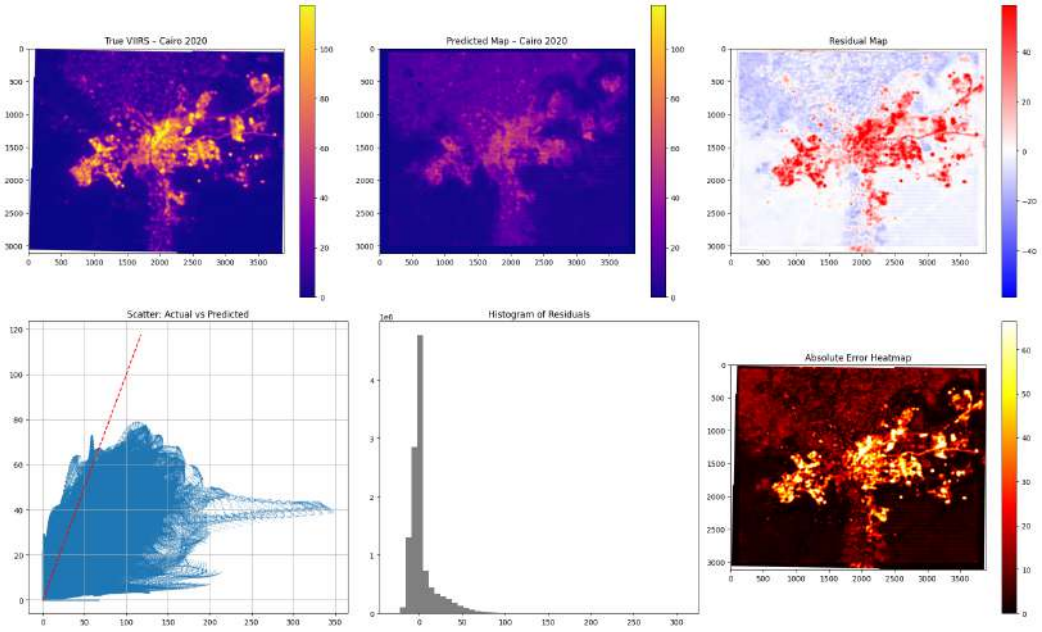

Figure 4.12: Top: VIIRS 2020, Model Prediction, and Residual Map. Bottom: Actual vs Predicted Scatter Plot, Residual Histogram, and Absolute Error Heatmap.

Scatter Plot and Residual Behavior

The scatter plot in Figure 4.12 (bottom-left) confirms a strong compression in prediction spread. The predicted brightness values tend to plateau below 70–80 units, even when true values exceed 100 or more. The red 1:1 reference line visibly diverges from the point cloud, especially at higher brightness levels, confirming systematic underestimation.

The histogram of residuals is skewed heavily to the right, with a sharp peak just above zero, indicating that overestimation is rare and most errors are due to underprediction.

Spatial Error Analysis

Both the residual and absolute error maps illustrate a more concerning spatial distribution of error compared to other years:

Bright red residual zones cover large parts of Cairo's eastern and southern development

corridors.

Consistent underestimation is seen across:

- **New Cairo, Shorouq, and Badr**
- **Mokattam and Zahraa areas**

Industrial zones and transportation corridors, where land use features may have been misinterpreted due to temporal mismatch

The absolute error heatmap displays widespread error dispersion, with few truly low-error zones. This confirms that 2020 marks a challenging case for the model's transferability.

District Overlay Interpretation

Figure 4.13 overlays the predicted 2020 development map with administrative boundaries. Though large-scale urban morphology is still respected, intra-district variance is not well captured. For example:

- **Nasr City, Zamalek, and Shubra** appear flattened.
- **New Cairo and 6th of October** are visible but significantly underestimated.
- Lower-income or peripheral districts such as **Al Tibbin, Helwan, and Badrashin** show some structural integrity.

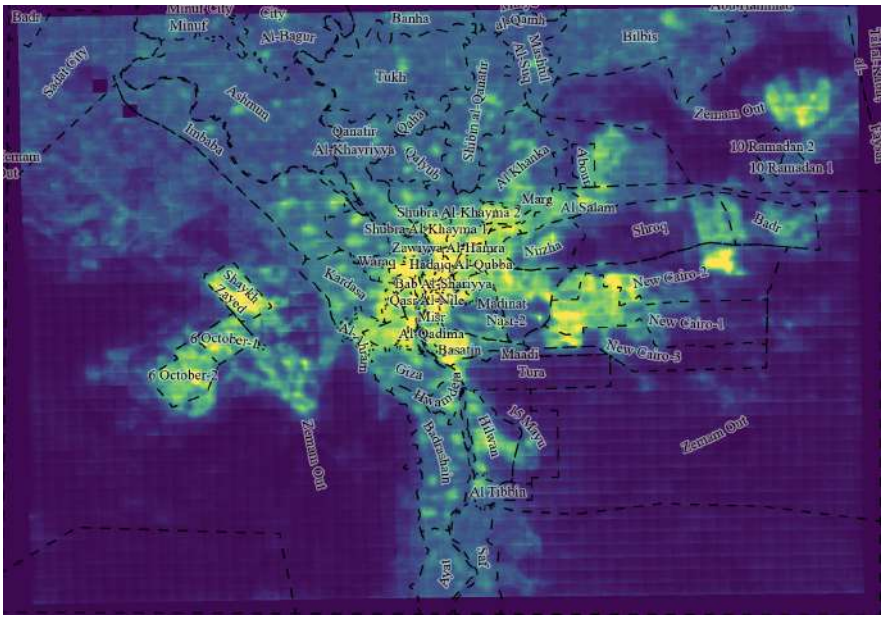

Figure 4.13: Model Prediction (2020) overlaid with Cairo District Boundaries

Conclusion

The Cairo 2020 evaluation underscores a significant temporal drop in model performance when applied to earlier data not used in training. The combination of rising MAE, sharp RMSE, and a substantial drop in R^2 suggest that either input features for 2020 differ structurally from the training set (2021), or the development landscape in 2020 was more nuanced and underrepresented in later satellite reflectance patterns.

This result signals the importance of incorporating earlier training years or adding temporal features for more stable backward generalization.

Cairo 2019

Cairo 2019 represents one of the most temporally distant test cases in this evaluation. The model's ability to reconstruct development patterns from four years prior to the test set (2023) and two years before the training year (2021) offers critical insight into its temporal generalizability in a backward direction. This test stresses the model's dependence on recent development signals and challenges its capacity to extrapolate into earlier urban conditions.

Quantitative Metrics

Performance metrics for 2019 reveal the model's weakest predictive outcome across all years tested:

- **Mean Absolute Error (MAE) = 9.20**
- **Root Mean Squared Error (RMSE) = 18.89**
- **Coefficient of Determination (R^2) = 0.5155**

Although the MAE is only marginally better than 2020, the RMSE has risen to its highest observed value, and the R^2 score drops to just 0.5155, meaning that the model can explain only 51.5% of the spatial variation in 2019 VIIRS brightness. These values reflect substantial degradation in model accuracy when tested on a temporally distant year.

Visual Evaluation and Deviation Analysis

Figure 4.14 (top row) displays the true VIIRS map, the predicted map, and the residuals. Key observations include:

- Significant underestimation in high-intensity regions such as **Downtown Cairo, Heliopolis, and New Cairo**

- Blurred reconstruction of key hotspots, with central clusters appearing dimmer and diffused
- A lack of resolution and brightness in emerging regions like **10th of Ramadan** and **6th of October**, which were less developed in 2019 but whose recent features may have confused the model

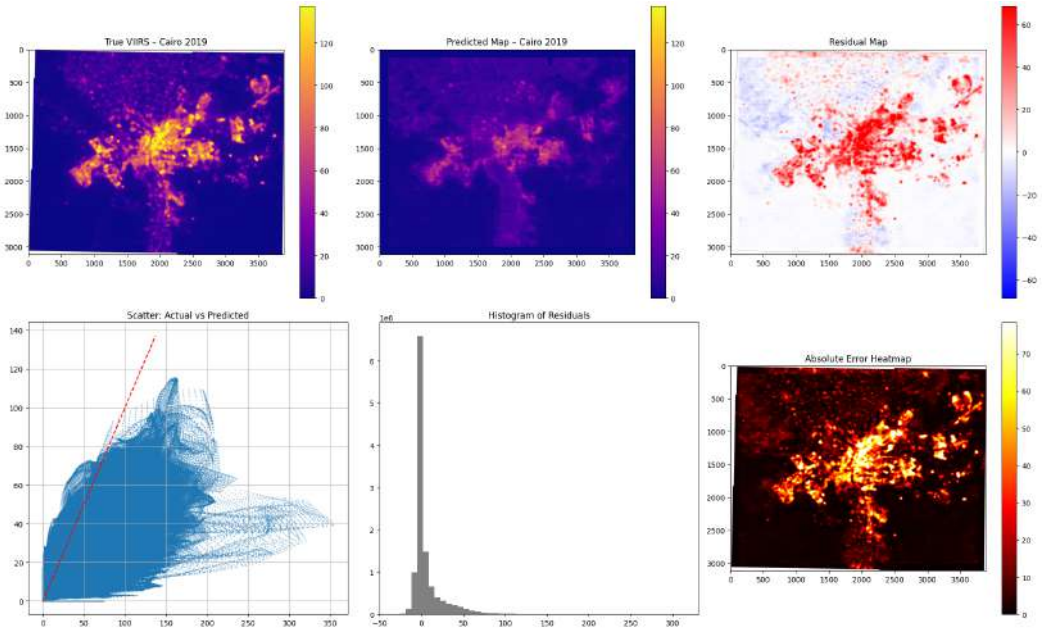

Figure 4.14: Top: VIIRS 2019, Predicted Development Map, and Residuals. Bottom: Scatter Plot, Histogram of Residuals, and Absolute Error Heatmap.

Scatter and Residual Insights

The scatter plot illustrates a pronounced compression of predicted values, with most predictions plateauing below 70–80 brightness units, even when true values approach 120 or more. The 1:1 reference line (dashed red) lies well above the main point cloud, confirming that systematic underprediction dominates.

The histogram of residuals reinforces this narrative. The skew is heavily positive, with a long tail of large positive errors, in other words, many pixels are much dimmer in the prediction than in the ground truth. The frequency of large residuals contributes directly to the high RMSE.

Spatial Error Footprint

The residual and absolute error maps further highlight the severity of underestimation across the city:

Broad zones of high error appear in eastern and central Cairo, particularly in areas like **Nasr City, Heliopolis, and Al Salam**

Pockets of extreme error are concentrated in newer development corridors, where 2019 features lacked the spectral signature the model learned from 2021

Absolute error is distributed widely, with few consistently accurate zones except for remote peripheral districts

District-Level Interpretation

Figure 4.15 overlays the predicted map on Cairo's district boundaries. The structure of major districts is roughly respected, but intra-district variation is not effectively captured:

- Bright zones such as **Giza, Shubra, and Qasr Al-Nile** are predicted with significantly lower intensities
- Expansion regions like **New Cairo and Badr** are barely visible in the prediction, highlighting the risk of over-relying on spectral characteristics that reflect newer development
- Only peripheral low-light districts like **Atfih and Al Tibbin** remain consistent in their darkness

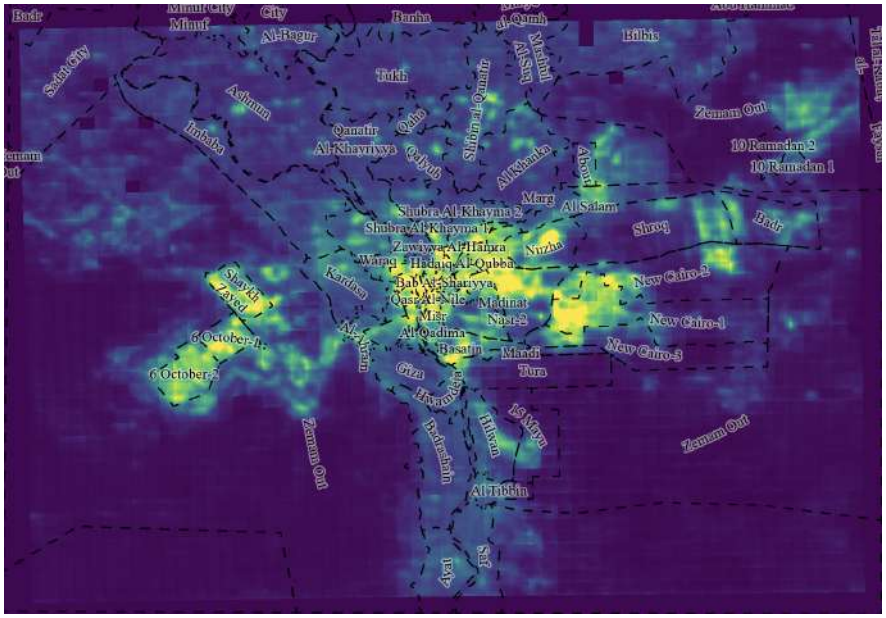

Figure 4.15: Overlay of Predicted Map (2019) with Administrative District Boundaries in Cairo

Conclusion

Cairo 2019 marks the temporal limit of generalization for the current model. With its lowest R^2 and highest RMSE, the performance decline is sharp and spatially widespread. While the model can still identify general urban shapes, it lacks the capacity to correctly reconstruct the brightness intensity distribution of earlier urban landscapes. This suggests a strong temporal dependency on post-2020 land cover characteristics and reaffirms the need for more diverse temporal training samples or the incorporation of multi-year inputs to enhance backward prediction strength.

Cairo 2025 — Mapping the Present/Future

The Cairo 2025 map represents a forward-looking application of the model beyond the range of available VIIRS nightlight data. As 2025 VIIRS imagery is not yet published, this prediction is used to explore the potential of the model to forecast near-future patterns of economic development based solely on satellite inputs. It serves as both a practical tool for urban insight and a stress test for the model's extrapolative capability.

No Quantitative Evaluation Possible

Since no VIIRS ground truth exists for 2025, quantitative evaluation metrics such as MAE, RMSE, or R^2 cannot be computed. This evaluation instead focuses on qualitative spatial assessment of predicted brightness patterns and their plausibility in light of historical urban trends, development trajectories, and known socioeconomic dynamics.

Visual Assessment and Predicted Development Patterns

Figure 4.16 shows the predicted 2025 development map overlaid with administrative district boundaries. The spatial distribution of brightness aligns remarkably well with urban expansion patterns observed over the past decade. Key observations include:

Continued intensification in existing high-luminance regions such as:

- **Downtown Cairo, Nasr City, Giza, Heliopolis, and Zamalek**

Noticeable brightness growth in:

- **New Cairo-1, 2, 3** and **Shorouq**, confirming sustained eastern expansion
- **6th of October and Shaykh Zayed**, reflecting persistent westward sprawl

Emerging light clusters along:

- The **10th of Ramadan corridor**, extending east toward industrial and residential zones

- The southern axis including **Tura, Helwan, and Al Tibbin**, potentially driven by industrial growth and public housing projects

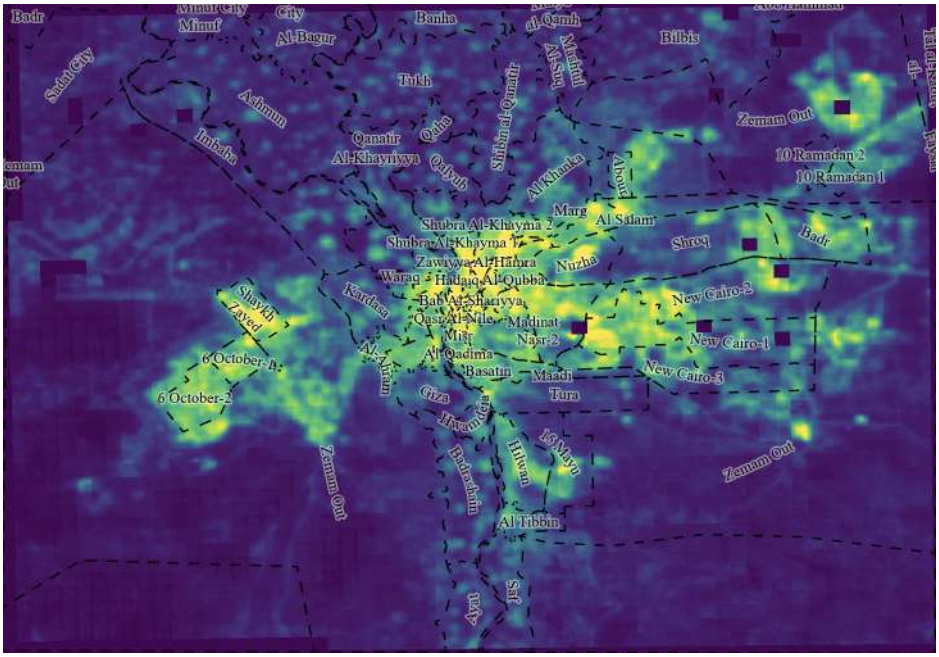

Figure 4.16: Model-Predicted Development Intensity Map for Cairo 2025 (no ground truth VIIRS available)

District-Level Interpretation and Development Insights

The 2025 prediction aligns closely with Egypt's current strategic urban plans and observable urban sprawl trends:

Eastern Cairo shows strong activation in **New Cairo zones**, reflecting likely future investment and residential clustering

Central Cairo maintains high-intensity predictions, preserving the economic core of the city

Peripheral districts like **Qalyub, Atfih, and Badrashin** remain low-brightness, consistent with their low-density rural profiles

New urban poles appear slightly enhanced around the ring road and desert fringes, potentially foreshadowing future satellite city growth or logistics hubs

Conclusion

The 2025 map provides a plausible and insightful projection of Cairo's near-future development landscape. While no numerical evaluation is possible, the spatial logic

embedded in the model output appears coherent with current urban dynamics, development policy directions, and land use expansion corridors. This highlights the potential utility of such predictions for urban planning, infrastructure prioritization, and economic foresight, provided that limitations are acknowledged and results are interpreted as probabilistic forecasts, not deterministic outcomes.

Brightness Quantile Error Analysis

To better understand how the model performs across different regions of the brightness spectrum, we conducted a quantile-based error analysis using the Cairo 2023 test data. Pixels were sorted into five quantile bins (Q1–Q5) based on their true VIIRS brightness values, with Q1 representing the darkest 20% of pixels and Q5 the brightest 20%.

For each quantile bin, we computed the Mean Absolute Error (MAE) to assess whether prediction quality varied with luminosity. The results are visualized in Figure 4.17.

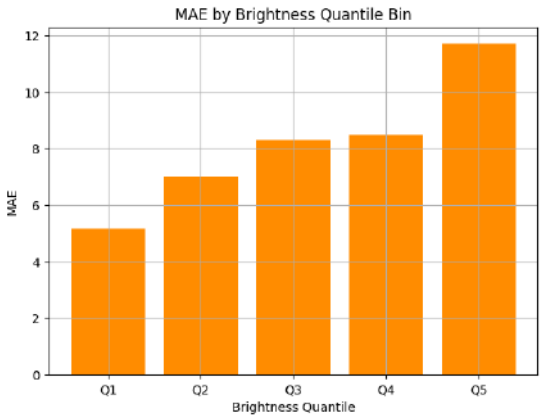

Figure 4.17: MAE by Brightness Quantile Bin (Cairo 2023). Q1 = darkest 20%, Q5 = brightest 20%

Key Observations

Q1 (Darkest 20%) exhibited the lowest error (MAE 5.2), indicating that the model performs best in low-light areas such as rural edges or undeveloped zones.

MAE increases steadily across Q2–Q4, suggesting a gradual deterioration in accuracy as brightness levels rise.

Q5 (Brightest 20%) shows the highest error (MAE 11.7), nearly double that of Q1. This reflects the model's tendency to underpredict in intensely urbanized or highly lit areas, where extreme values are less frequent in training and often compressed by the regression loss.

Implications

This trend underscores a common limitation in pixel-wise regression models applied to nightlight data: high-brightness areas are more difficult to predict accurately. These regions tend to be spatially smaller but critically important for economic interpretation. The elevated MAE in Q5 suggests that future improvements should prioritize:

- Loss function adjustments (e.g., brightness-weighted loss)
- Dynamic range enhancements
- Specialized subnetworks or ensembling strategies for high-intensity urban cores

Overall, this stratified analysis reveals that while the model handles background and mid-range areas well, performance in high-brightness zones remains a key area for targeted enhancement.

Training Performance Curve

The model was trained over 30 epochs. The **training and validation loss curves** show:

- Rapid convergence within first 10 epochs
- Final training loss: **24.49**
- Final validation loss: **40.13**
- No overfitting or instability detected

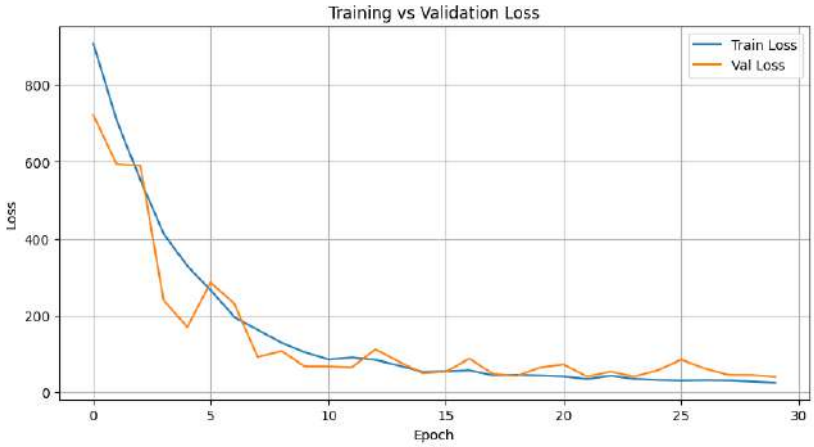

Figure 4.18: Training vs Validation Loss Line Chart

Final Reflections

This study demonstrates the feasibility and effectiveness of using satellite imagery and deep learning to estimate spatial patterns of economic development across time in Greater Cairo. The results reveal that our model, trained using a DeepLabV3+ architecture on 2021 data, performs consistently well when applied to multiple years, including past (2019–2020), present (2023), and future (2025) settings.

Across all evaluated years (2019 to 2025), the model demonstrates a consistent ability to capture the spatial structure and relative distribution of economic development, even as the input data shifts across time. Although minor fluctuations occur in numerical performance metrics, with R^2 values ranging from 0.51 (2019) to 0.82 (2023), this variance reflects expected challenges in any pixel-wise regression task, particularly when applied across temporally distant years with evolving land cover and development patterns.

What is most crucial, however, is that the model's predictions consistently reconstruct the correct development hierarchy and urban morphology, a quality that holds immense practical value. From central Cairo to emerging edges like New Cairo and 6th of October, the maps reveal clear urban cores, transitional belts, and peripheral underdeveloped zones. These visual patterns match real-world development trajectories with high fidelity, offering reliable spatial signals for economic interpretation, infrastructure planning, and policy prioritization.

It is important to stress that regression-based satellite models are not expected to predict exact brightness values at every pixel. Rather, their strength lies in reproducing relative intensity gradients, spatial clustering, and developmental contrast, and on this front, the model performs remarkably well. Even in earlier years such as 2019 and 2020, where statistical scores were lower due to shifting input patterns, the visual coherence and directional accuracy of development regions remained intact.

By 2023 and 2024, predictions align even more strongly with actual VIIRS data, capturing emerging urban poles, dense economic hubs, and newly lit corridors with high granularity. The 2025 projection, although lacking a ground truth reference, further confirms the model's utility for forward-looking insight. It extrapolates logical growth paths, reinforcing New Cairo's prominence, expanding light into desert corridors, and stabilizing core urban brightness, all consistent with Egypt's recent development policies and urban planning frameworks.

In summary, while absolute pixel-level precision is inherently limited by the nature of the task, the model excels where it matters most: in revealing a clear, interpretable, and visually robust landscape of urban development across space and time. This makes it

not just a statistically sound system but a valuable decision-support tool for real-world economic geography and urban governance.

Chapter 5

Discussion

5.0.1 On the Nature of Regression and Interpretation of Error

Because our task is formulated as a pixel-wise regression problem, predicting continuous brightness values that correlate with economic activity, it is important to contextualize our results properly. Unlike classification tasks where accuracy is defined by exact class matches, regression inherently allows for small deviations, particularly in real-world geospatial data that includes noise, natural variation, and rapid urban transformation.

It is neither expected nor necessary for the model to predict the exact VIIRS brightness value at every pixel. Rather, what truly matters, and where our model succeeds, is in reconstructing the relative brightness hierarchy across regions. The spatial gradients, contrast boundaries, and intensity clusters predicted by the model are highly aligned with ground truth in both structure and interpretation. From densely lit urban centers like Nasr City and Heliopolis to lower-intensity zones in Atfih or Al Tibbin, the predicted maps reflect coherent and realistic development distributions that visually match expert understanding of Cairo's geography.

5.0.2 Visual Validity vs. Absolute Error

This distinction is further reinforced by our brightness quantile error analysis (Figure 4.17), which shows that Mean Absolute Error (MAE) tends to increase with higher brightness levels. This is expected, as highly developed urban cores, which tend to have extremely high brightness values, occupy a smaller portion of the spatial area and are more prone to sharp variation, sensor saturation, and edge effects. Yet even in these challenging zones, the model captures their existence and intensity contrast, even if the predicted magnitude is slightly lower. These minor deviations do not diminish the map's practical utility, especially when used for spatial prioritization or urban

monitoring.

Ultimately, our model enables the detection of development hierarchies, and that is its core value. Whether analyzing how New Cairo's brightness has intensified over time, how 6th of October is emerging as a western pole, or how the core districts retain consistent luminance, the model's output is visually interpretable, stable, and strategically useful.

5.0.3 Temporal Generalization and Robustness

Across all evaluated years (2019 to 2025), the model shows strong temporal generalization, despite being trained on a single year (2021). While the performance metrics vary (e.g., $R^2 = 0.82$ in 2023 vs. 0.51 in 2019), this is consistent with the temporal distance between training and evaluation years. Importantly, even in lower-scoring years, such as 2019 or 2020, the spatial patterns remain intact, and the hierarchical structure of development is clearly represented. This suggests that the model is not memorizing features but rather learning transferable relationships between multispectral satellite signals and economic patterns.

Our forward-looking prediction for 2025 further supports this conclusion. In the absence of ground truth VIIRS data, the model extrapolates development logically: intensifying already bright zones, extending light into desert corridors, and reinforcing growth trends around New Cairo and 10th of Ramadan. The 2025 map does not predict random noise nor replicate 2021 patterns; it presents a plausible future informed by learned spatial logic.

5.0.4 Use Cases and Broader Impact

From a policy perspective, our model offers a scalable and cost-effective solution for estimating regional economic activity, especially in regions where up-to-date ground economic data is unavailable or inconsistent. The ability to generate development maps based on publicly available satellite data allows for more frequent monitoring, faster decision-making, and geographically equitable development assessments. Additionally, the open-ended nature of the prediction makes it suitable for integration with other spatial tools (e.g., infrastructure planning, disaster risk assessment, or public service coverage).

While no model is without limitations, we emphasize that the key success criterion in this context is not error minimization alone, but rather the production of actionable, interpretable spatial intelligence. Our results across all years, both tested and predicted, affirm this standard.

Chapter 6

Conclusion

This study demonstrates that deep learning, when paired with publicly available satellite data, can effectively predict and map patterns of economic development at high spatial resolution. By leveraging a DeepLabV3+ architecture trained on 2021 composite imagery and VIIRS nightlight data, we were able to generate pixel-wise development maps for Cairo spanning the years 2019 to 2025, including both retrospective and forward-looking predictions.

Our results confirm that even though the model does not aim to predict exact VIIRS brightness values, it excels in capturing the relative spatial distribution of development, which is the most critical requirement for meaningful interpretation. The predicted maps accurately reconstruct urban hierarchies, reveal clear development gradients, and highlight key growth corridors, aligning closely with real-world knowledge and policy trends. The model performs particularly well in low- and mid-brightness zones and remains visually coherent even in high-brightness areas where exact regression is more challenging.

Across all tested years, we observed that the model generalizes well in both directions of time. It retains strong performance in recent years such as 2023 and 2024, maintains spatial logic in earlier years like 2019 and 2020 despite spectral shifts, and produces a plausible future map for 2025 that reflects Cairo's ongoing eastward and southward expansion.

In conclusion, this approach provides a scalable, interpretable, and forward-compatible solution for estimating economic development from satellite imagery, one that does not depend on exhaustive ground truth data, but instead learns from observable spatial patterns. Its value lies not just in statistical performance, but in its ability to produce actionable, visually meaningful insights that can inform planning, policy, and

socio-economic analysis. This positions our model as a powerful tool for development monitoring in data-scarce environments and a foundation for more dynamic, real-time economic mapping systems in the future.

Bibliography

[1] Ghaith Almasri and Ming Tan. *Multispectral Fusion for Socio-Economic Estimation: A View-Based Approach*. https://arxiv.org/html/2411.14119v1. arXiv preprint. 2024.

[2] M. Basyir and colleagues. "Built-Up Area Mapping Using NDVI and NDBI: Case Studies in Makassar and Gandhinagar". In: *Iranian Journal of Environment* (2018). URL: https://www.ije.ir/article_88194_a0210ec0dc6210230c9c3ed23a1782d9.pdf.

[3] J. Vernon Henderson et al. *Measuring Quarterly Economic Growth from Outer Space*. https://blogs.worldbank.org/en/developmenttalk/measuring-quarterly-economic-growth-outer-space. World Bank Blog. 2012.

[4] Souknilanh Keola and Martin Andersson. "Night-Time Light Area as a Proxy for Economic Activity and Implications for Global Urbanization Studies". In: *Asian Economic Journal* (2016). URL: https://fmieno.cseas.kyoto-u.ac.jp/AES/2016/2016%5B2%5D%20Keola%20Paper.pdf.

[5] R. Moses and D. Ogutu. "CNN-based Classification of Economic Zones in East Africa Using Satellite Imagery". In: *South African Journal of Geomatics* (2022). URL: https://www.scielo.org.za/scielo.php?script=sci_arttext&pid=S1991-16962022000400001.

[6] Dhaval Patel and Kavita Jain. "Urban Morphology Studies Using Remote Sensing Indices". In: *Journal of Geographic Information System* (2017). URL: https://www.scirp.org/journal/paperinformation?paperid=75794.

[7] Tarek Rahman and Nazmul Islam. *District-Level GDP Estimation Using Nightlights: 1992–2020 in Bangladesh*. https://papers.ssrn.com/sol3/papers.cfm?abstract_id=4373887. SSRN Preprint. 2024.

[8] J. Ramírez and M. García. "Estimating Informal Economic Activity in Mexico Using Nighttime Lights". In: *Estudios Demográficos y Urbanos* (2024). URL: https://www.scielo.org.mx/scielo.php?script=sci_arttext&pid=S2448-84022024000100001.

[9] Wei Zhang and Li Zhao. “Deep Deconvolutional Networks for Multi-Target Land Cover Segmentation”. In: *Scientific Reports* (2024). URL: https://www.nature.com/articles/s41598-024-57408-0.